Méthode d'éléments de frontière

Marc Bonnet

UMA (Dept. of Appl. Math.), POems, UMR 7231 CNRS-INRIA-ENSTA
32, boulevard Victor, 75739 PARIS cedex 15, France
mbonnet@ensta.fr

École doctorale MODES *Methodes numériques avancées*, 28 mars 2013

http://uma.ensta.fr/~mbonnet/enseignement.html

Outline

Electrostatics

- Well-known, and simple, physical setting
- Allows to introduce important concepts of integral equation formulations with a clear physical meaning
- Said concepts will generalize to other settings (elasticity, electromagnetics...)
- Also helpful later for a physical understanding of the fast multipole method (FMM)

Electrostatics: discrete charged particles

- Coulomb interaction force:

$$\mathbf{F}_{12} = \frac{q_1 q_2}{4\pi\varepsilon} \frac{1}{r^2} \hat{\mathbf{r}}_{12}$$

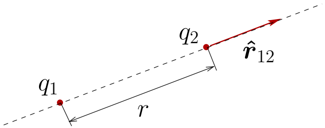

- Electrostatic field:

$$\mathbf{F}_{12} = q_2 \mathbf{E}_{12}, \quad \mathbf{E}_{12} = \frac{q_1}{4\pi\varepsilon} \frac{1}{r^2} \hat{\mathbf{r}}_{12}$$

- Electrostatic potential:

$$\mathbf{E}_{12} = -\boldsymbol{\nabla}_2 V, \quad V = \frac{q_1}{4\pi\varepsilon} \frac{1}{r}$$

(with ε: **permittivity** of the medium (material constant))

Electrostatics: continuous charge distributions

- Continuous charge distribution: $\boxed{\mathrm{d}q = \varrho \, \mathrm{d}V}$:

$$\boxed{\mathbf{E}(\mathbf{x}) = \frac{1}{4\pi\varepsilon} \int_V \frac{\varrho(\boldsymbol{\xi})}{r^2} \hat{\mathbf{r}} \, \mathrm{d}V_\xi} \qquad \mathbf{r} = \boldsymbol{\xi} - \mathbf{x}, \quad r = \|\mathbf{r}\|, \quad \hat{\mathbf{r}} = \mathbf{r}/r$$

- Gauss theorem:

$$\boxed{\operatorname{div} \mathbf{E} = \frac{\varrho}{\varepsilon}}$$

- Poisson equation (Gauss theorem with $\mathbf{E} = -\boldsymbol{\nabla} V$):

$$\boxed{\Delta V + \frac{\varrho}{\varepsilon} = 0}$$

Electrostatics: continuous charge distributions

Proof of Gauss theorem:

$$\begin{aligned}\int_V \operatorname{div}\mathbf{E}\,\mathrm{d}V &= \int_{\partial V}\mathbf{E}\cdot\mathbf{n}\,\mathrm{d}S\\ &= \frac{1}{4\pi\varepsilon}\int_V\Big\{\int_{\partial V}\frac{1}{r^2}\,(\hat{\mathbf{r}}\cdot\mathbf{n}(\mathbf{x}))\,\mathrm{d}S_x\Big\}\varrho(\boldsymbol{\xi})\,\mathrm{d}V_\xi\\ &= \frac{1}{4\pi\varepsilon}\int_V\Theta(\boldsymbol{\xi})\varrho(\boldsymbol{\xi})\,\mathrm{d}V_\xi\end{aligned}$$

where $\Theta(\boldsymbol{\xi})$ is the **solid angle** of the (closed) surface ∂V from origin $\boldsymbol{\xi}$:

$$\Theta(\boldsymbol{\xi}) = 4\pi\ \ (\boldsymbol{\xi}\in V), \qquad \Theta(\boldsymbol{\xi}) = 0\ \ (\boldsymbol{\xi}\in\mathbb{R}^3\setminus\bar{V})$$

Hence:

$$\int_V \operatorname{div}\mathbf{E}\,\mathrm{d}V = \int_V \frac{\varrho}{\varepsilon}\,\mathrm{d}V$$

Since this is true for any domain V, one has $\operatorname{div}\mathbf{E} = \varrho/\varepsilon$, i.e. the Gauss theorem holds.

Electrostatic volume potential

The electrostatic volume potential results from the superposition of electric fields generated by elementary charges $\varrho \, \mathrm{d}V$ distributed in a volume V:

$$\mathcal{V}[\varrho, V](\mathbf{x}) = \frac{1}{4\pi\varepsilon} \int_V \frac{\varrho(\boldsymbol{\xi})}{r} \, \mathrm{d}V_\xi$$

As already seen, $\mathcal{V}[\varrho, V]$ satisfies the Poisson equation:

$$\Delta\mathcal{V}[\varrho, V] + \frac{\varrho}{\varepsilon} = 0 \quad (\mathbf{x} \in V), \qquad \Delta\mathcal{V}[\varrho, V] = 0 \quad (\mathbf{x} \in \mathbb{R}^3 \setminus \bar{V})$$

Properties of electrostatic volume potentials

- The volume integral is weakly singular (i.e. singular, but integrable) for $\mathbf{x} \in V$, so that $\mathcal{V}[\varrho, V]$ is well-defined inside the charged domain V: one has
$$\mathrm{d}V_x = r^2 \, \mathrm{d}r \, \mathrm{d}\Theta = O(r^2)$$
- $\mathcal{V}[\varrho, V]$ is continuous everywhere, and in particular across the boundary ∂V.

Electrostatic single-layer potential

The electrostatic single-layer potential results from the superposition of electric fields generated by elementary charges $\varrho\,\mathrm{d}S$ distributed on a surface S:

$$\mathcal{S}[\varrho, S](\mathbf{x}) = \frac{1}{4\pi\varepsilon}\int_S \frac{\varrho(\boldsymbol{\xi})}{r}\,\mathrm{d}S_\xi$$

$\mathcal{S}[\varrho, S]$ is harmonic outside of S:

$$\Delta\mathcal{S}[\varrho, S] = 0 \quad (\mathbf{x}\in\mathbb{R}^3\setminus S)$$

Properties of electrostatic single-layer potentials

- The surface integral is weakly singular (i.e. singular, but integrable) for $\mathbf{x}\in S$, so that $\mathcal{S}[\varrho, S]$ is well-defined on the charged surface V: one has

$$\mathrm{d}S_x = r\,\mathrm{d}r\;\mathrm{d}\theta = O(r)$$

- $\mathcal{S}[\varrho, S]$ is continuous everywhere, and in particular across S.

Electrostatic double-layer potential

The electrostatic double-layer potential is the limiting case of the superposition of two single-layer potentials of (i) arbitrary close supports $S^{\pm}$, (ii) opposite charge density, (iii) finite dipolar moment q:

$$\mathcal{D}[q,S](\mathbf{x}) = \lim_{h\to 0} \mathcal{S}[\varrho_h, S^+](\mathbf{x}) + \mathcal{S}[-\varrho_h, S^-](\mathbf{x})$$

with

$$\lim_{h\to 0}[h\varrho_h](\mathbf{x}) = q(\mathbf{x})$$

(note: q is analogous to a concentrated moment)

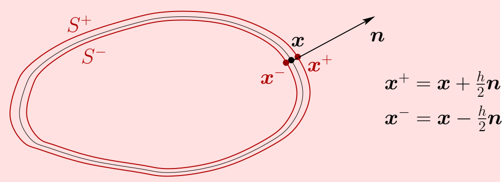

Performing the limit $h \to 0$, one finds:

$$\mathcal{D}[q,S](\mathbf{x}) = -\frac{1}{4\pi\varepsilon} \int_S \frac{1}{r^2} \hat{\mathbf{r}} \cdot \mathbf{n}(\boldsymbol{\xi}) \, q(\boldsymbol{\xi}) \, \mathrm{d}S_{\xi}$$

Electrostatic double-layer potential

$$\mathcal{D}[q,S](\mathbf{x}) = -\frac{1}{4\pi\varepsilon}\int_S \frac{1}{r^2}\hat{\mathbf{r}}\cdot\mathbf{n}(\boldsymbol{\xi})\; q(\boldsymbol{\xi})\,\mathrm{d}S_\xi$$

Properties of electrostatic double-layer potentials

- $\mathcal{D}[q,S]$ is harmonic outside of S:

$$\Delta\mathcal{D}[q,S] = 0 \quad (\mathbf{x}\in\mathbb{R}^3\setminus S)$$

- The surface integral is weakly singular (i.e. singular, but integrable) for $\mathbf{x}\in S$, so that $\mathcal{D}[q,S]$ is well-defined on the charged surface V.
  This is not obvious and stems from

$$\mathrm{d}S_x = r\,\mathrm{d}r\,\mathrm{d}\theta = O(r) \quad \text{and} \quad \frac{1}{r^2}\hat{\mathbf{r}}\cdot\mathbf{n} = O(\frac{1}{r})$$

- $\mathcal{D}[q,S]$ is discontinuous across S, with

$$\mathcal{D}[q,S](\mathbf{x}^+) - \mathcal{D}[q,S](\mathbf{x}^-) = q(\mathbf{x})$$

Electrostatic potentials: comments

(a) Electrostatic potentials have a clear physical meaning as the potential fields associated with volume, surface or dipolar charge distributions.

(b) Electrostatic potentials, as mathematical constructs, define harmonic fields for arbitrary choices of supports V, S and densities ϱ, q.

(c) As we will shortly see, **any** harmonic function can be expressed in terms of such potentials.

Physical problems governed by the Laplace or Poisson equation

Poisson equation:

$$\Delta u + b = 0 \ \text{(on } \Omega\text{)} \quad + \text{unspecified well-posed BCs}$$

(Laplace equation if $b = 0$)

- Electrostatics (u: electrostatic potential);
- Potential fluid flow (u: velocity potential);
- Thermal equilibrium (u: temperature);
- Torsion (u: warping function defined on 2-D section of shaft)

...

Reciprocity identity and integral representation

$$\Delta u + b = 0 \ \ \text{(in } \Omega\text{)} \quad + \text{unspecified well-posed BCs}$$

Integral representation of u based on two ingredients:

(i) Reciprocity identity:

$$\int_{\Omega} (u\Delta v - v\Delta u)\,\mathrm{d}V = \int_{\partial\Omega} (uv_{,n} - vu_{,n})\,\mathrm{d}V \qquad (u_{,n} \equiv \boldsymbol{\nabla} u \cdot \mathbf{n})$$

(ii) Fundamental solution:

$$\Delta G(\mathbf{x}, \cdot) + \delta(\cdot - \mathbf{x}) = 0 \ \ \text{(in } \mathcal{O} \supset \Omega\text{)}$$

Choosing $v = G(\mathbf{x}, \cdot)$ in (i) yields the integral representation formula:

$$u(\mathbf{x}) = \int_{\Omega} G(\mathbf{x}, \boldsymbol{\xi}) b(\boldsymbol{\xi})\,\mathrm{d}V_{\xi} + \int_{\partial\Omega} \big(G(\mathbf{x}, \boldsymbol{\xi}) u_{,n}(\boldsymbol{\xi}) - G_{,n}(\mathbf{x}, \boldsymbol{\xi}) u(\boldsymbol{\xi}) \big)\,\mathrm{d}S_{\xi} \quad (\mathbf{x} \in \Omega)$$

Full-space fundamental solution ($\mathcal{O} = \mathbb{R}^3$):

$$G(\mathbf{x}, \boldsymbol{\xi}) = \frac{1}{4\pi r} \quad (r = \|\boldsymbol{\xi} - \mathbf{x}\|)$$

Volume and single-layer potentials

- The **single-layer potential** $\mathcal{S}$ solves the Laplace equation in $\mathbb{R}^3 \setminus \partial\Omega$, where

$$\mathcal{S}[\varphi, \partial\Omega](\mathbf{x}) := \int_{\partial\Omega} G(\mathbf{x}, \boldsymbol{\xi})\varphi(\boldsymbol{\xi}) \,\mathrm{d}S_\xi$$

The **volume potential** $\mathcal{V}$ solves the Poisson equation, where

$$\mathcal{V}[b, \Omega](\mathbf{x}) := \int_{\Omega} G(\mathbf{x}, \boldsymbol{\xi})b(\boldsymbol{\xi}) \,\mathrm{d}V_\xi$$

- Continuity across $\partial\Omega$ (with $[\![f]\!] := f^+ - f^-$):

$$[\![\mathcal{V}(\mathbf{x})]\!] = 0, \quad [\![\mathcal{S}(\mathbf{x})]\!] = 0, \qquad (\mathbf{x} \in \partial\Omega)$$

Double-layer potentials

- The following potential solve the Laplace equation in $\mathbb{R}^3 \setminus \partial\Omega$:

$$\mathcal{D}[\psi, \partial\Omega](\mathbf{x}) := \int_{\partial\Omega} G_{,n}(\mathbf{x}, \boldsymbol{\xi})\psi(\boldsymbol{\xi})\,\mathrm{d}S_\xi \qquad \text{(double-layer potential)}$$

- Jump relation:

$$[\![\mathcal{D}(\mathbf{x})]\!] = \psi(\mathbf{x}) \qquad (\mathbf{x} \in \partial\Omega)$$

- Boundary traces of double-layer potential:

$$\begin{aligned} \mathcal{D}[\psi, \partial\Omega](\mathbf{x}^-) &= (c(\mathbf{x}) - 1)\psi(\mathbf{x}) + \mathcal{D}[\psi, \partial\Omega](\mathbf{x}), \\ \mathcal{D}[\psi, \partial\Omega](\mathbf{x}^+) &= \mathcal{D}[\psi, \partial\Omega](\mathbf{x}^-) + \psi(\mathbf{x}) \end{aligned}$$

with the definitions ($\Theta(\mathbf{x})$: solid angle of Ω seen from $\mathbf{x} \in \partial\Omega$):

$$\mathcal{D}[\psi, \partial\Omega](\mathbf{x}) := \int_{\partial\Omega} G_{,n}(\mathbf{x}, \boldsymbol{\xi})\psi(\boldsymbol{\xi})\,\mathrm{d}S_\xi, \quad c(\mathbf{x}) = \Theta(\mathbf{x})/(4\pi) \qquad (\mathbf{x} \in \partial\Omega)$$

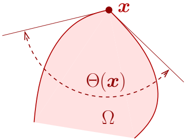

When $\partial\Omega$ is smooth at $\mathbf{x}$ (the usual case), $\Theta(\mathbf{x}) = 2\pi$ and $c(\mathbf{x}) = 1/2$

Integral representation as sum of potentials

Expressing the integral representation formula in terms of potentials yields

$$u(\mathbf{x}) = \mathcal{V}[b, \Omega](\mathbf{x}) + \mathcal{S}[u_{,n}, \partial\Omega](\mathbf{x}) - \mathcal{D}[u, \partial\Omega](\mathbf{x})$$

Any harmonic function is representable as a single-layer, or a double-layer potential, or a linear combination of both.

Any solution of the Poisson equation is representable as a sum of the volume potential of density b and arbitrary surface potentials.

Singular integral equations

Boundary integral equations are obtained as the limiting situation when $\mathbf{z} \in \Omega \to \mathbf{z} \in \partial\Omega$ of integral representations:

$$\begin{aligned} u(\mathbf{x}) &= \lim_{\mathbf{z}\to\mathbf{x}} u(\mathbf{z}) \\ &= \lim_{\mathbf{z}\to\mathbf{x}} \Big[\mathcal{V}[b,\Omega](\mathbf{z}) + \mathcal{S}[u_{,n},\partial\Omega](\mathbf{z}) - \mathcal{D}[u,\partial\Omega](\mathbf{z}) \Big] \\ &= \mathcal{V}[b,\Omega](\mathbf{x}) + \mathcal{S}[u_{,n},\partial\Omega](\mathbf{x}) - \mathcal{D}[u,\partial\Omega](\mathbf{x}) + (1-c(\mathbf{x}))u(\mathbf{x}) \end{aligned}$$

to obtain:

$$\boxed{c(\mathbf{x})u(\mathbf{x}) + \mathcal{D}[u,\partial\Omega](\mathbf{x}) - \mathcal{S}[u_{,n},\partial\Omega](\mathbf{x}) = \mathcal{V}[b,\Omega](\mathbf{x}) \qquad (\mathbf{x} \in \partial\Omega)}$$

i.e. (in expanded form)

$$\boxed{c(\mathbf{x})u(\mathbf{x}) + \int_{\partial\Omega} \big(G_{,n}(\mathbf{x},\boldsymbol{\xi})u(\boldsymbol{\xi}) - G(\mathbf{x},\boldsymbol{\xi})u_{,n}(\boldsymbol{\xi}) \big) \, \mathrm{d}S_{\xi} = \int_{\Omega} G(\mathbf{x},\boldsymbol{\xi})b(\boldsymbol{\xi}) \, \mathrm{d}V_{\xi}}$$

$$(\mathbf{x} \in \partial\Omega)$$

Outline of the boundary integral equation method

$$c(\mathbf{x})u(\mathbf{x}) + \mathcal{D}[u,\partial\Omega](\mathbf{x}) - \mathcal{S}[u_{,n},\partial\Omega](\mathbf{x}) = \mathcal{V}[b,\Omega](\mathbf{x}) \qquad (\mathbf{x}\in\partial\Omega)$$

1. Insert given boundary data;
   Solve for the remaining boundary unknown
2. Then, invoke integral representation for evaluation of u (and related quantities, e.g. $\boldsymbol{\nabla} u$) at interior points

Example ($\partial\Omega = S_u \cup S_{\text{q}}$, with $u = u^{\text{D}}$ on S_u and $u_{,n} = q^{\text{D}}$ on S_{q}):

1. Solve for $u|_{S_{\text{q}}}$ and $u_{,n}|_{S_u}$ the integral equation system

$$\begin{aligned}
&c(\mathbf{x})u(\mathbf{x}) + \mathcal{D}[u,S_{\text{q}}](\mathbf{x}) - \mathcal{S}[u_{,n},S_u](\mathbf{x}) \\
&\qquad = -\mathcal{D}[u^{\text{D}},S_u](\mathbf{x}) + \mathcal{S}[q^{\text{D}},S_{\text{q}}](\mathbf{x}) + \mathcal{V}[b,\Omega](\mathbf{x}) && (\mathbf{x}\in S_{\text{q}}) \\
&\mathcal{D}[u,S_{\text{q}}](\mathbf{x}) - \mathcal{S}[u_{,n},S_u](\mathbf{x}) \\
&\qquad = -c(\mathbf{x})u^{\text{D}}(\mathbf{x}) - \mathcal{D}[u^{\text{D}},S_u](\mathbf{x}) + \mathcal{S}[q^{\text{D}},S_{\text{q}}](\mathbf{x}) + \mathcal{V}[b,\Omega](\mathbf{x}) && (\mathbf{x}\in S_u)
\end{aligned}$$

2. Integral representation:

$$u(\mathbf{x}) = \mathcal{V}[b,\Omega](\mathbf{x}) + \mathcal{S}[u_{,n},\partial\Omega](\mathbf{x}) - \mathcal{D}[u,\partial\Omega](\mathbf{x})$$

Fundamental solution, Green's function

$$\Delta u + b = 0 \ \ (\text{in } \Omega) \qquad u = u^{\text{D}} \ \ (\text{on } S_u), \quad u_{,n} = q^{\text{D}} \ \ (\text{on } S_{\text{q}})$$

- Fundamental solution (again):

$$\Delta G(\mathbf{x},\cdot) + \delta(\cdot - \mathbf{x}) = 0 \ \ (\text{in } \mathcal{O} \supset \Omega)$$

  i.e. **any** field induced in Ω by a unit point source placed at $\mathbf{x} \in \Omega$
- Green's function: fundamental solution with homogeneous BCs on $\partial\Omega$:

$$\begin{aligned} \Delta_{\xi} \mathcal{G}(\mathbf{x},\cdot) + \delta(\cdot - \mathbf{x}) &= 0 \ \ (\text{in } \Omega) \\ \mathcal{H}(\mathbf{x},\cdot) := \boldsymbol{\nabla}\mathcal{G}(\mathbf{x},\cdot)\cdot\mathbf{n}(\cdot) &= 0 \ \ (\text{on } S_{\text{q}}), \\ \mathcal{G}(\mathbf{x},\cdot) &= 0 \ \ (\text{on } S_u) \end{aligned}$$

- Fundamental solution $\longrightarrow$ boundary unknowns u (on S_{q}) and $u_{,n}$ (on S_u) (boundary integral equation needed)
- Green's function $\longrightarrow$ **explicit** integral representation formula (boundary integral equation **not** needed)

$$u(\mathbf{x}) = \int_{\Omega} \mathcal{G}(\mathbf{x},\boldsymbol{\xi}) b(\boldsymbol{\xi}) \, \text{d}V_{\xi} + \int_{S_{\text{q}}} \mathcal{G}(\mathbf{x},\boldsymbol{\xi}) q^{\text{D}}(\boldsymbol{\xi}) \, \text{d}S_{\xi} - \int_{S_u} \mathcal{H}(\mathbf{x},\boldsymbol{\xi}) u^{\text{D}}(\boldsymbol{\xi}) \, \text{d}S_{\xi} \ \ (\mathbf{x} \in \Omega)$$

Green's functions (Laplace): half-space

"Method of images":

$$\mathcal{G}(\mathbf{x},\boldsymbol{\xi}) = G(\mathbf{x},\boldsymbol{\xi}) + G(\mathbf{x}^{\text{sym}},\boldsymbol{\xi})$$ Neumann BC on free surface

$$\mathcal{G}(\mathbf{x},\boldsymbol{\xi}) = G(\mathbf{x},\boldsymbol{\xi}) - G(\mathbf{x}^{\text{sym}},\boldsymbol{\xi})$$ Dirichlet BC on free surface

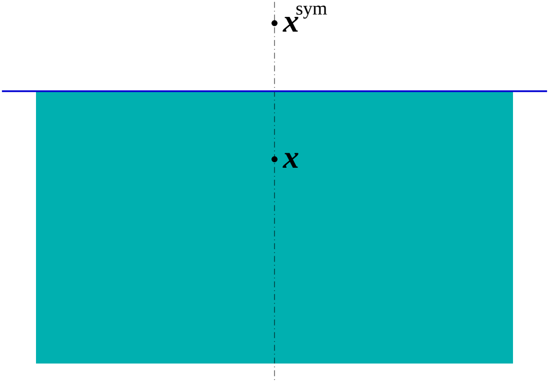

Green's functions (Laplace): sphere

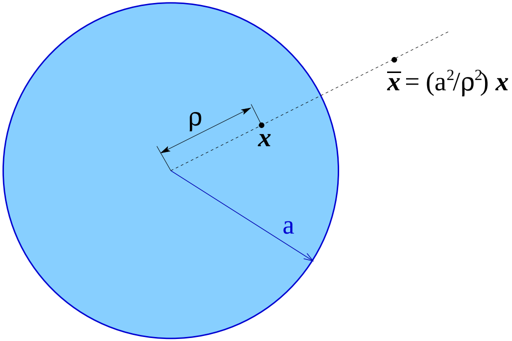

$$\mathcal{G}(\mathbf{x}, \boldsymbol{\xi}) = \frac{1}{4\pi}\left(\frac{1}{r} - \frac{a}{\rho}\frac{1}{\bar{r}}\right) \quad \text{(Dirichlet BC on surface)}$$

Indirect boundary integral equations:

- Seek solutions of Laplace equation using potentials:

$$u(\mathbf{x}) = \mathcal{S}[\varphi, \partial\Omega](\mathbf{x}) + \mathcal{D}[\psi, \partial\Omega](\mathbf{x}) \quad (\mathbf{x} \in \Omega)$$

Dirichlet problem ($u = u^{\text{D}}$ on $\partial\Omega$) using double-layer potential:

$$-c(\mathbf{x})\psi(\mathbf{x}) + \mathcal{D}[\psi, \partial\Omega](\mathbf{x}) = u^{\text{D}}(\mathbf{x}) \quad (\mathbf{x} \in \partial\Omega)$$

Neumann problem ($u_{,n} = p^{\text{D}}$ on $\partial\Omega$) using single-layer potential:

$$c(\mathbf{x})\varphi(\mathbf{x}) - \partial_{n(x)}\mathcal{S}[\varphi, \partial\Omega](\mathbf{x}) = p^{\text{D}}(\mathbf{x}) \quad (\mathbf{x} \in \partial\Omega)$$

- Seek solutions of Poisson equation using potentials:

$$u(\mathbf{x}) = \mathcal{V}[b, \partial\Omega](\mathbf{x}) + \mathcal{S}[\varphi, \partial\Omega](\mathbf{x}) + \mathcal{D}[\psi, \partial\Omega](\mathbf{x}) \quad (\mathbf{x} \in \Omega)$$

Reciprocity identity and integral representation

- Additive decomposition of strain into elastic and initial (e.g. thermal, plastic, visco-plastic) parts (assuming infinitesimal strain):

$$\boldsymbol{\varepsilon} = \boldsymbol{\varepsilon}^{\mathsf{E}} + \boldsymbol{\varepsilon}^{\mathsf{I}} \qquad \text{where} \quad \boldsymbol{\sigma} = \boldsymbol{\mathcal{C}} : \boldsymbol{\varepsilon}^{\mathsf{E}}$$

- Constitutive equation ($\boldsymbol{\mathcal{C}}$: fourth-order tensor of elastic moduli):

$$\boldsymbol{\sigma} = \boldsymbol{\mathcal{C}} : (\boldsymbol{\varepsilon} - \boldsymbol{\varepsilon}^{\mathsf{I}})$$

- For isotropic elasticity (μ: shear modulus, ν: Poisson ratio):

$$\mathcal{C}_{ijk\ell} = \mu \Big[\frac{2\nu}{1-2\nu} \delta_{ij}\delta_{k\ell} + (\delta_{ik}\delta_{j\ell} + \delta_{i\ell}\delta_{jk}) \Big]$$

- Governing field equation for unknown displacement field $\mathbf{u}(\boldsymbol{\xi})$:

$$C_{ijab}(u_{a,bj} - \varepsilon^{\mathsf{I}}_{ab,j}) + b_i = 0 \qquad (\boldsymbol{\xi} \in \Omega)$$

Elastostatic fundamental solution

Kelvin fundamental solution: unit point force applied at $\mathbf{x} \in \mathbb{R}^3$ along k-direction in unbounded elastic medium, i.e.:

$$C_{ijab} U^k_{a,bj} + \delta(\cdot - \mathbf{x})\delta_{ik} = 0 \qquad (\boldsymbol{\xi} \in \mathbb{R}^3)$$

$$U^k_i(\mathbf{x},\boldsymbol{\xi}) = \frac{1}{16\pi\mu(1-\nu)} \frac{1}{r} \big[\hat{r}_i \hat{r}_k + (3-4\nu)\delta_{ik} \big]$$

$$\Sigma^k_{ij}(\mathbf{x},\boldsymbol{\xi}) = -\frac{1}{8\pi(1-\nu)} \frac{1}{r^2} \big[3\hat{r}_i \hat{r}_k \hat{r}_j + (1-2\nu)(\delta_{ik}\hat{r}_j + \delta_{jk}\hat{r}_i - \delta_{ij}\hat{r}_k) \big] \qquad \mathbf{x},\boldsymbol{\xi} \in \mathbb{R}^3$$

$$T^k_i(\mathbf{x},\boldsymbol{\xi}) = \Sigma^k_{ij}(\mathbf{x},\boldsymbol{\xi}) n_j(\boldsymbol{\xi})$$

$$\big(\; r = |\boldsymbol{\xi} - \mathbf{x}| , \qquad \hat{r}_i = (\xi_i - x_i)/r \; \big)$$

Reciprocity identity and integral representation

Governing field equation for unknown displacement field $\mathbf{u}(\boldsymbol{\xi})$:

$$\int_\Omega \big\{ C_{ijab}(u_{a,bj} - \varepsilon^{\mathsf{I}}_{ab,j}) + b_i \big\} \times U_i^k(\mathbf{x},\boldsymbol{\xi}) \, \mathrm{d}V_\xi = 0 \qquad (1)$$

Governing field equation for fundamental solution:

$$\int_\Omega \big\{ C_{ijab} U^k_{a,bj} + \delta(\boldsymbol{\xi} - \mathbf{x})\delta_{ik} \big\} \times u_i(\boldsymbol{\xi}) \, \mathrm{d}V_\xi = 0 \qquad (2)$$

Performing (1)-(2) and invoking the divergence identity, one obtains the **integral representation formula** of the displacement:

$$u_k(\mathbf{x}) = \int_{\partial\Omega} \Big\{ U_i^k(\mathbf{x},\boldsymbol{\xi}) t_i(\boldsymbol{\xi}) - T_i^k(\mathbf{x},\boldsymbol{\xi}) u_i(\boldsymbol{\xi}) \Big\} \, \mathrm{d}S_\xi + \int_\Omega \Big\{ U_i^k(\mathbf{x},\boldsymbol{\xi}) b_i(\boldsymbol{\xi}) + \Sigma_{ij}^k(\mathbf{x},\boldsymbol{\xi}) \varepsilon^{\mathsf{I}}_{ij}(\boldsymbol{\xi}) \Big\} \, \mathrm{d}V_\xi$$

- **Partially unknown** contribution of $\partial\Omega$ (BC + unknown trace)
- **Known** contribution of Ω (if ε^{I} is known beforehand)

Displacement boundary integral equation

Limiting process as $\mathbf{x} \in \Omega \longrightarrow \mathbf{z} \in \partial\Omega$ in integral representation:

$$u_k(\mathbf{x}) = \int_{\partial\Omega} \Big\{ U_i^k(\mathbf{x},\boldsymbol{\xi}) t_i(\boldsymbol{\xi}) - T_i^k(\mathbf{x},\boldsymbol{\xi}) u_i(\boldsymbol{\xi}) \Big\} \, \mathrm{d}S_x + \int_{\Omega} \Big\{ U_i^k(\mathbf{x},\boldsymbol{\xi}) b_i(\boldsymbol{\xi}) + \Sigma_{ij}^k(\mathbf{x},\boldsymbol{\xi}) \varepsilon_{ij}^{\mathrm{I}}(\boldsymbol{\xi}) \Big\} \, \mathrm{d}V_\xi$$

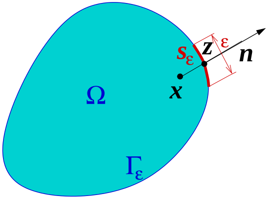

Non-integrable singularity of $\mathbf{T}^k(\mathbf{x},\boldsymbol{\xi})$:

- Limit to the boundary approach
- Direct approach using exclusion neighbourhood of $\mathbf{z}$
- Indirect regularization approach

Displacement boundary integral equation

Integral equation, singular form:

$$\frac{1}{2}u_k(\mathbf{x}) + \text{P.V.}\int_{\partial\Omega} T_i^k(\mathbf{x},\boldsymbol{\xi})u_i(\boldsymbol{\xi})\,\mathrm{d}S_x - \int_{\partial\Omega} U_i^k(\mathbf{x},\boldsymbol{\xi})t_i(\boldsymbol{\xi})\,\mathrm{d}S_x = \int_{\Omega}\Big\{U_i^k(\mathbf{x},\boldsymbol{\xi})b_i(\boldsymbol{\xi}) + \Sigma_{ij}^k(\mathbf{x},\boldsymbol{\xi})\varepsilon^{\mathrm{I}}_{ij}(\boldsymbol{\xi})\Big\}\,\mathrm{d}V_\xi$$

Integral equation, regularized form:

$$\int_{\partial\Omega}\big\{\,T_i^k(\mathbf{x},\boldsymbol{\xi})[u_i(\boldsymbol{\xi}) - u_i(\mathbf{x})] - U_i^k(\mathbf{x},\boldsymbol{\xi})t_i(\boldsymbol{\xi})\big\}\,\mathrm{d}S_x = \int_{\Omega}\Big\{U_i^k(\mathbf{x},\boldsymbol{\xi})b_i(\boldsymbol{\xi}) + \Sigma_{ij}^k(\mathbf{x},\boldsymbol{\xi})\varepsilon^{\mathrm{I}}_{ij}(\boldsymbol{\xi})\Big\}\,\mathrm{d}V_\xi$$

- Both forms require $\mathbf{u}\in C^{0,\alpha}$ (otherwise process $\mathbf{x}\in\Omega\to\mathbf{z}\in\partial\Omega$ breaks down)
- Numerical implementation based on (well-documented) singular element integration methods.
- Boundary-only formulations in the absence of body forces and initial strains.
- Treatments (double / multiple reciprocity methods) sometimes allow to convert domain integrals with $\mathbf{b},\varepsilon^{\mathrm{I}}$ into boundary integrals.

Volume, single-layer and double-layer elastic potentials

- Volume potential (prescribed body forces):

$$\mathcal{V}_k^b[\mathbf{b},\Omega](\mathbf{x}) = \int_\Omega U_i^k(\mathbf{x},\boldsymbol{\xi}) b_i(\boldsymbol{\xi}) \, \mathrm{d}V_\xi$$

(displacement field created in $\mathbb{R}^3$ by $\mathbf{b}$ given on Ω)

- Volume potential (prescribed initial strains):

$$\mathcal{V}_k^\varepsilon[\boldsymbol{\varepsilon}^\mathsf{I},\Omega](\mathbf{x}) = \int_\Omega \Sigma_{ij}^k(\mathbf{x},\boldsymbol{\xi}) \varepsilon_{ij}^\mathsf{I}(\boldsymbol{\xi}) \, \mathrm{d}V_\xi$$

(displacement field created in $\mathbb{R}^3$ by $\boldsymbol{\varepsilon}^\mathsf{I}$ given on Ω)

- Single-layer elastic potential:

$$\mathcal{S}[\boldsymbol{\varphi},\partial\Omega]_k(\mathbf{x}) = \int_{\partial\Omega} U_i^k(\mathbf{x},\boldsymbol{\xi}) \varphi_i(\boldsymbol{\xi}) \, \mathrm{d}S_x$$

- Double-layer elastic potential:

$$\mathcal{D}[\boldsymbol{\psi},\partial\Omega]_k(\mathbf{x}) = \int_{\partial\Omega} T_i^k(\mathbf{x},\boldsymbol{\xi}) \psi_i(\boldsymbol{\xi}) \, \mathrm{d}S_x$$

Green's tensor (elasticity): half-space (Mindlin solution)

$$U_i^k(\mathbf{x},\boldsymbol{\xi}) = \frac{1}{16\pi\mu(1-\nu)}\left\{ \frac{\kappa}{r}\delta_{ik} + \frac{1}{\bar{r}}\delta_{ik} + \frac{r_{,i}r_{,k}}{r} + \kappa\frac{\bar{r}_{,i}\bar{r}_{,k}}{\bar{r}} + \frac{2x_3y_3}{\bar{r}^3}\left[\delta_{ik} - 3\bar{r}_{,i}\bar{r}_{,k}\right] + \frac{\chi}{\bar{r}(1+\bar{r}_{,3})}\left[\delta_{ik} - \frac{\bar{r}_{,i}\bar{r}_{,k}}{1+\bar{r}_{,3}}\right]\right\}$$

$$U_3^k(\mathbf{x},\boldsymbol{\xi}) = \frac{1}{16\pi\mu(1-\nu)}\left\{ \frac{r_{,3}r_{,k}}{r} + \kappa\frac{\bar{r}_{,k}}{\bar{r}}\left[\bar{r}_{,3} - \frac{2x_3}{\bar{r}}\right] - \frac{6x_3y_3}{\bar{r}^3}\bar{r}_{,3}\bar{r}_{,k} + \chi\frac{\bar{r}_{,k}}{\bar{r}(1+\bar{r}_{,3})}\right\}$$

$$U_i^3(\mathbf{x},\boldsymbol{\xi}) = \frac{1}{16\pi\mu(1-\nu)}\left\{ \frac{r_{,i}r_{,3}}{r} + \kappa\frac{\bar{r}_{,k}}{\bar{r}}\left[\bar{r}_{,3} - \frac{2x_3}{\bar{r}}\right] + \frac{6x_3y_3}{\bar{r}^3}\bar{r}_{,i}\bar{r}_{,3} - \chi\frac{\bar{r}_{,i}}{\bar{r}(1+\bar{r}_{,3})}\right\}$$

$$U_3^3(\mathbf{x},\boldsymbol{\xi}) = \frac{1}{16\pi\mu(1-\nu)}\left\{ \frac{\kappa}{r} + \frac{1+\chi}{\bar{r}} + \frac{r_{,3}^2}{r} + \kappa\frac{\bar{r}_3\bar{r}_3}{\bar{r}} - \frac{2x_3y_3}{\bar{r}^3}\left[1 - 3\bar{r}_{,3}\bar{r}_{,3}\right]\right\}$$

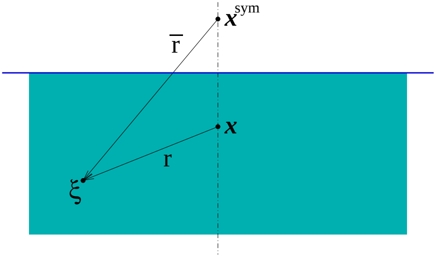

$(\kappa = 3-4\nu,\ \chi = 4(1-\nu)(1-2\nu))$

Green's tensors (elasticity)

- Full-space (Kelvin):
  exact solutions (within full-space idealization):
  $\longrightarrow$ Response to arbitrary eigenstrain distribution:

$$u_k(\mathbf{x}) = \int_\Omega \Sigma^k_{ij}(\mathbf{x}, \boldsymbol{\xi}) \varepsilon^{\text{I}}_{ij}(\boldsymbol{\xi}) \, \mathrm{d}V_\xi$$

  $\longrightarrow$ Elastic ellipsoidal inhomogeneity (Eshelby problem), using equivalent-inclusion approach
- Half-space with free surface (Mindlin, 1936), Boussinesq as special case:
  exact solutions (within half-space idealization):
  $\longrightarrow$ Soil mechanics and geotechnics;
  $\longrightarrow$ Contact mechanics (Hertz solution, Galin formulae)
- Two perfectly-bonded half spaces (Rongved, 1955) – closed form
- Elastic layer between two parallel planar free surfaces (Benitez and Rosakis 1987) – integral transform

Reciprocity identity and integral representation

$$\Delta u + k^2 u = 0 \ \text{(in } \Omega) \quad + \text{unspecified well-posed BCs}$$

Time-harmonic problems ($u(\boldsymbol{\xi}, t) = \text{Re}[u(\boldsymbol{\xi})e^{-\mathrm{i}\omega t}]$); wavenumber $k = \omega/c$.
e.g. linear acoustics (u: pressure, $(\mathrm{i}\rho\omega)^{-1}\boldsymbol{\nabla} u$: velocity)

- Reciprocity identity:

$$\int_{\Omega} (u\Delta v - v\Delta u)\,\mathrm{d}V = \int_{\partial\Omega} (uv_{,n} - vu_{,n})\,\mathrm{d}V \qquad (u_{,n} \equiv \boldsymbol{\nabla} u \cdot \mathbf{n})$$

- Fundamental solution (full space):

$$\Delta G(\mathbf{x}, \cdot) + k^2 G(\mathbf{x}, \cdot) + \delta(\cdot - \mathbf{x}) = 0 \ \text{(in } \mathcal{O} \supset \Omega)$$

$$G(\mathbf{x}, \boldsymbol{\xi}) = \frac{e^{\mathrm{i}k\|\boldsymbol{\xi}-\mathbf{x}\|}}{4\pi\|\boldsymbol{\xi}-\mathbf{x}\|} \qquad (\mathcal{O} = \mathbb{R}^3)$$

Integral representation:

$$u(\mathbf{x}) = \int_{\partial\Omega} \Big\{ G(\mathbf{x}, \boldsymbol{\xi}) u_{,n}(\boldsymbol{\xi}) - G_{,n}(\mathbf{x}, \boldsymbol{\xi}) u(\boldsymbol{\xi}) \Big\}\,\mathrm{d}S_{\xi} \quad (\mathbf{x} \in \Omega)$$

Singular integral equation

- Dynamic (Helmholtz) and static (Laplace) fundamental solutions have same singularity:

$$G(\mathbf{x},\boldsymbol{\xi}) = \frac{e^{\mathrm{i}k\|\boldsymbol{\xi}-\mathbf{x}\|}}{4\pi\|\boldsymbol{\xi}-\mathbf{x}\|} = \frac{1}{4\pi\|\boldsymbol{\xi}-\mathbf{x}\|} + O(1) \qquad (\boldsymbol{\xi}\to\mathbf{x})$$

- Limit to the boundary (or other) approach yields the same free term $c(\mathbf{x})$ as with Laplace problems
- **Singular integral equation:**

$$c(\mathbf{x})u(\mathbf{x}) + \int_{\partial\Omega} \Big\{ G_{,n}(\mathbf{x},\boldsymbol{\xi})u(\boldsymbol{\xi}) - G(\mathbf{x},\boldsymbol{\xi})u_{,n}(\boldsymbol{\xi}) \Big\}\,\mathrm{d}S_{\xi} = 0 \quad (\mathbf{x}\in\partial\Omega)$$

- Singular integrals: invoke methods for handling **static** singular kernels:

$$\int_{\partial\Omega} G_{,n}(\mathbf{x},\boldsymbol{\xi})u(\boldsymbol{\xi})\,\mathrm{d}S_{\xi} = \int_{\partial\Omega} \Big\{ G_{,n}(\mathbf{x},\boldsymbol{\xi}) - G_{,n}(\mathbf{x},\boldsymbol{\xi};\omega=0) \Big\} u(\boldsymbol{\xi})\,\mathrm{d}S_{\xi} + \int_{\partial\Omega} G_{,n}(\mathbf{x},\boldsymbol{\xi};\omega=0)u(\boldsymbol{\xi})\,\mathrm{d}S_{\xi}$$

Half-space problems

Method of images still applicable:

$$\mathcal{G}(\mathbf{x},\boldsymbol{\xi}) = G(\mathbf{x},\boldsymbol{\xi}) + G(\mathbf{x}^{\text{sym}},\boldsymbol{\xi}) \qquad \text{Neumann BC on free surface}$$

$$\mathcal{G}(\mathbf{x},\boldsymbol{\xi}) = G(\mathbf{x},\boldsymbol{\xi}) - G(\mathbf{x}^{\text{sym}},\boldsymbol{\xi}) \qquad \text{Dirichlet BC on free surface}$$

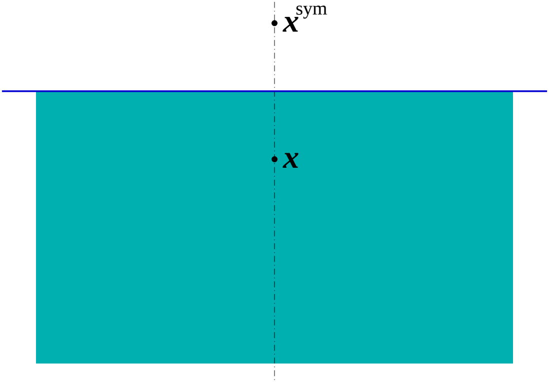

Unbounded media

Wave equations (scalar, elastic, Maxwell...) frequently employed for media idealized as **unbounded**

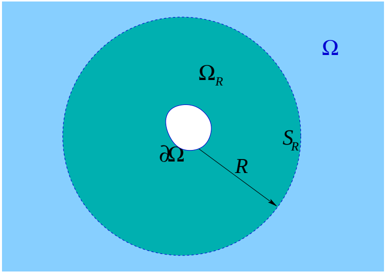

Limiting case as $R \longrightarrow \infty$ of

$$c(\mathbf{x})u(\mathbf{x}) + \left\{ \int_{S_R} + \int_{\partial\Omega} \right\} \big(G_{,n}(\mathbf{x},\boldsymbol{\xi})u(\boldsymbol{\xi}) - G(\mathbf{x},\boldsymbol{\xi})u_{,n}(\boldsymbol{\xi}) \big) \, \mathrm{d}S_\xi = 0 \quad (\mathbf{x} \in \partial\Omega)$$

Unbounded media, radiation conditions

Integral equation

$$c(\mathbf{x})u(\mathbf{x}) + \int_{\partial\Omega} \big(G_{,n}(\mathbf{x},\boldsymbol{\xi})u(\boldsymbol{\xi}) - G(\mathbf{x},\boldsymbol{\xi})u_{,n}(\boldsymbol{\xi}) \big) \,\mathrm{d}S_{\xi} = 0 \quad (\mathbf{x} \in \partial\Omega)$$

valid if u satisfies a **radiation condition** at infinity:

- Integral form:

$$\lim_{R\to\infty} \int_{S_R} \big(G_{,n}(\mathbf{x},\boldsymbol{\xi})u(\boldsymbol{\xi}) - G(\mathbf{x},\boldsymbol{\xi})u_{,n}(\boldsymbol{\xi}) \big) \,\mathrm{d}S_{\xi} = 0$$

- Local form, sufficient, known as Sommerfeld condition:

$$\boldsymbol{\nabla} u \cdot \hat{\mathbf{x}} - iku = o(\|\mathbf{x}\|^{-1}) \qquad \|\mathbf{x}\| \longrightarrow \infty$$

  (Sommerfeld is known to imply $u = o(1)$, i.e. decay of u at infinity)

The radiation condition is satisfied by $G(\mathbf{x},\cdot)$, and consequently also by

- The fundamental solution
- Volume, single-layer, double-layer potentials
- Integral representation formula

Scattering of incident waves by hard obstacles

- Governing equations (hard obstacle[s])

$$\Delta u + k^2 u = 0 \qquad \text{in } \Omega$$
$$\boldsymbol{\nabla} u \cdot \mathbf{n} = 0 \qquad \text{on } \partial\Omega \quad \text{(no normal velocity, i.e. hard obstacle)}$$

- **Known** incident wave (or 'free-field') u^{F}; radiation conditions not assumed (e.g. plane wave):

$$\Delta u^{\mathsf{F}} + k^2 u^{\mathsf{F}} = 0 \quad (\text{in } \mathbb{R}^3)$$

- **Decomposition:**

$$\boxed{u = u^{\mathsf{F}} + v = \text{incident} + \text{scattered},} \qquad + \text{ radiation conditions for } v$$

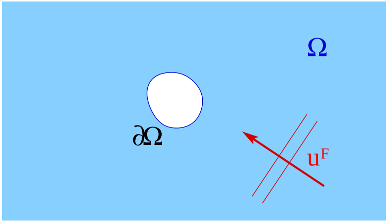

Scattering of incident waves by hard obstacles

- Scattered field verifies integral equation (by virtue of radiation cnds):

$$c(\mathbf{x})v(\mathbf{x}) + \int_{\partial\Omega} \Big\{ G_{,n}(\mathbf{x},\boldsymbol{\xi})v(\boldsymbol{\xi}) - G(\mathbf{x},\boldsymbol{\xi})v_{,n}(\boldsymbol{\xi}) \Big\} \, \mathrm{d}S_{\xi} = 0 \qquad \text{(a)}$$

- Free-field verifies **integral equation for interior of scatterer**:

$$[c(\mathbf{x}) - 1]u^{\mathrm{F}}(\mathbf{x}) + \int_{\partial\Omega} \Big\{ G_{,n}(\mathbf{x},\boldsymbol{\xi})u^{\mathrm{F}}(\boldsymbol{\xi}) - G(\mathbf{x},\boldsymbol{\xi})u^{\mathrm{F}}_{,n}(\boldsymbol{\xi}) \Big\} \, \mathrm{d}S_{\xi} = 0 \quad \text{(b)}$$

- **Simplified** integral equation formulation (a)+(b) in terms of total field:

$$\boxed{c(\mathbf{x})u(\mathbf{x}) + \int_{\partial\Omega} G_{,n}(\mathbf{x},\boldsymbol{\xi})u(\boldsymbol{\xi}) \, \mathrm{d}S_{\xi} = u^{\mathrm{F}}(\mathbf{x})}$$

Fictitious eigenfrequencies

BIE formulations for **exterior** problems break down when ω is an eigenfrequency for a certain **interior** problem.

Example:

- Direct BIE formulation for exterior Neumann problem (scattering by rigid obstacle):

$$c(\mathbf{x})u(\mathbf{x}) + \int_{\partial\Omega} G_{,n}(\mathbf{x},\boldsymbol{\xi})u(\boldsymbol{\xi})\,\mathrm{d}S_\xi = u^{\mathrm{F}}(\mathbf{x}) \qquad \text{(a)}$$

- Indirect BIE formulation (using a double-layer potential representation) for interior homogeneous Dirichlet problem (using same normal as (a)):

$$c(\mathbf{x})\psi(\mathbf{x}) + \int_{\partial\Omega} G_{,n}(\mathbf{x},\boldsymbol{\xi})\psi(\boldsymbol{\xi})\,\mathrm{d}S_\xi = 0 \qquad \text{(b)}$$

- (b) has non-trivial solutions if ω is a Dirichlet eigenvalue.
- Therefore, so does (a) as the governing integral operator is the same

Remedies include:

(i) enforcing an extra set of integral identities at interior points;
(ii) combining (with complex coefficients) two BIE formulations having different eigenvalues (see treatment in Pyl, Clouteau, Degrande 2004)

Scattering of incident waves by penetrable obstacles

- **Penetrable** inclusion $(\rho^\star(\boldsymbol{\xi}), c^\star(\boldsymbol{\xi})$ and with definitions $\beta = \rho/\rho^\star,\ \gamma = c/c^\star)$:

$$(\Delta + k^2)u = 0 \quad (\text{in } \Omega \setminus \bar{B}) \qquad (\Delta + \gamma^2 k^2)u^\star = 0 \quad (\text{in } B)$$
$$u = u^\star, \qquad u_{,n} = \beta u^\star_{,n} \qquad (\text{on } \partial B)$$

- Domain integral equation of Lippman-Schwinger type (proof: combine reciprocity identities written on B for $u^\star$ and on $\mathbb{R}^3 \setminus B$ for $u - u^{\mathsf{F}}$):

$$u(\mathbf{x}) + \int_B \big[(\beta - 1)\boldsymbol{\nabla} G(\mathbf{x},\boldsymbol{\xi})\boldsymbol{\nabla} u(\boldsymbol{\xi}) + (1 - \beta\gamma^2)k^2 G(\mathbf{x},\boldsymbol{\xi})u(\boldsymbol{\xi})\big] \, \mathrm{d}V_\xi = u^{\mathsf{F}}(\mathbf{x})$$

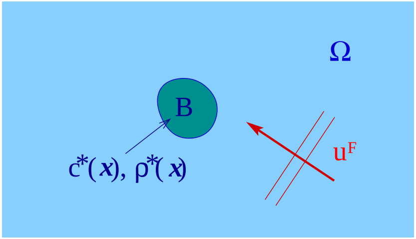

Linear elastodynamics

Governing field equation:

$$\mathrm{div}\,(\mathcal{C}:\varepsilon[\mathbf{u}]) + \rho\omega^2\mathbf{u} + \mathbf{b} = 0 \qquad (\text{in } \Omega)$$

Fundamental solution (full space):

$$U_i^k(\mathbf{x},\boldsymbol{\xi}) = \frac{1}{k_S^2\mu}\Big[\,(\delta_{qs}\delta_{ik} - \delta_{qk}\delta_{is})\frac{\partial}{\partial x_q}\frac{\partial}{\partial \xi_s}G(\|\mathbf{x}-\boldsymbol{\xi}\|;k_{\mathrm{S}}) + \frac{\partial}{\partial x_i}\frac{\partial}{\partial \xi_k}G(\|\mathbf{x}-\boldsymbol{\xi}\|;k_{\mathrm{P}})\,\Big]$$

$$G(z;k) = \frac{e^{\mathrm{i}kz}}{4\pi z}, \quad k_{\mathrm{S}}^2 = \frac{\rho\omega^2}{\mu}, \quad k_{\mathrm{P}}^2 = \frac{1-2\nu}{2(1-\nu)}k_{\mathrm{S}}^2$$

Radiation conditions for unbounded media, local form:

$$\left.\begin{aligned} \boldsymbol{\sigma}[\mathbf{u}^{\mathrm{P}}]\cdot\hat{\mathbf{x}} - \mathrm{i}\rho\omega c_{\mathrm{P}} &= o(\|\mathbf{x}\|^{-1}) \\ \boldsymbol{\sigma}[\mathbf{u}^{\mathrm{S}}]\cdot\hat{\mathbf{x}} - \mathrm{i}\rho\omega c_{\mathrm{S}} &= o(\|\mathbf{x}\|^{-1}) \end{aligned}\right\} \quad \|\mathbf{x}\| \longrightarrow \infty$$

Interpolation

- Partition $\partial\Omega$ into elements (possibly curvilinear and with curvilinear edges):

$$\partial\Omega = \cup_{e=1}^{\mathrm{N}_e} E_e$$

- Isoparametric representation (most commonly used) of $\partial\Omega$ and unknown ϕ:

$$\mathbf{x} = \sum_{q=1}^{n(e)} N_q(\mathbf{a})\mathbf{x}^q$$

$$\phi(\mathbf{x}) = \sum_{q=1}^{n(e)} N_q(\mathbf{a})\phi^q$$

$$(\mathbf{a} = (a_1, a_2) \in \Delta_e)$$

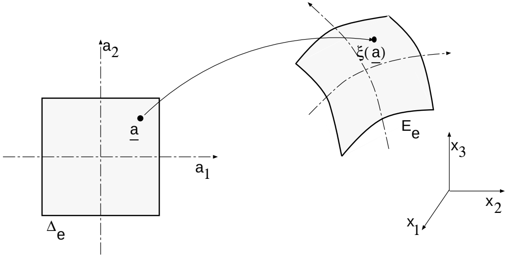

- Connectivity table:

$Q(e,q)$ global number of q-th node of E_e $\quad (1 \leq e \leq \mathrm{N}_e, 1 \leq q \leq n(e))$

- Isoparametric interpolation: $N = \mathrm{N}_{\mathrm{N}}$ (for scalar problems).
(with N_{N}: number of nodes and N: number of unknown nodal DOFs)

Collocation BEM

Sample integral equation (Laplace + Dirichlet, direct or single-layer formulation):

$$\int_{\partial\Omega} G(\mathbf{x},\boldsymbol{\xi})\varphi(\boldsymbol{\xi})\,\mathrm{d}S_\xi = b(\mathbf{x}) \qquad (\mathbf{x}\in\partial\Omega)$$

- Principle: enforce integral equation at the $\mathrm{N_N}$ nodes $\mathbf{x}=\mathbf{x}^1,\ldots,\mathbf{x}^{\mathrm{N_N}}$.
- Leads to linear system of equations

$$\boxed{\mathbf{A}\varphi = \mathbf{b}} \qquad (\mathbf{A}\in\mathbb{R}^{N\times N},\ \mathbf{b}\in\mathbb{R}^{N})$$

  where

$$A_{PQ} = \sum_{e\in I(Q)} \int_{\Delta_e} G(\mathbf{x}^P,\boldsymbol{\xi}(\mathbf{a}))N_Q(\mathbf{a})J(\mathbf{a})\,\mathrm{d}\mathbf{a} \qquad (1\le P,Q\le N)$$

$$b_P = b(\mathbf{x}^P)$$

- Matrix **A square, fully-populated, invertible, non-symmetric** obtained by assembly of element matrices

$$\mathbf{A}^e(\mathbf{x}^P)\in\mathbb{R}^{1,n(e)} = \left[\int_{\Delta_e} G(\mathbf{x}^P,\boldsymbol{\xi}(\mathbf{a}))N_q(\mathbf{a})J(\mathbf{a})\,\mathrm{d}\mathbf{a}\right]_{1\le q\le n(e)}$$

Evaluation of element integrals

$$\mathbf{A}^e(\mathbf{x}^P) \in \mathbb{R}^{1,n(e)} = \left[\int_{\Delta_e} G(\mathbf{x}^P, \boldsymbol{\xi}(\mathbf{a})) N_q(\mathbf{a}) J(\mathbf{a}) \, \mathrm{d}\mathbf{a} \right]_{1 \leq q \leq n(e)}$$

- If $\mathbf{x}^P \notin E_e$ (nonsingular element integral): Gaussian quadrature

$$\mathbf{A}^e(\mathbf{x}^P) \approx \sum_{g=1}^{G} w_g \, G(\mathbf{x}^P, \boldsymbol{\xi}(\mathbf{a}_g)) N_q(\mathbf{a}_g) J(\mathbf{a}_g)$$

- If $\mathbf{x}^P \in E_e$ (singular element integral): specialized treatment:
  - Weakly singular integrals ($O(r^{-1})$ kernel in 3-D) removed by suitable transformaation of parametric coordinates $\mathbf{a}$
  - Strongly singular integrals ($O(r^{-2})$ in 3-D) either
    - **(i)** recast into weakly singular integrals using regularization techniques
    - **(ii)** evaluated directly as Cauchy principal values
  - For simple element shapes and interpolations (e.g. 3-noded isoparametric triangle), analytic singular integration available

Galerkin BEM

Example (simplest): solve Dirichlet problem for Laplace equation using single-layer potential

$$\forall\tilde{\varphi}\in H^{-1/2}(\partial\Omega),\quad \text{find}\quad \varphi\in H^{-1/2}(\partial\Omega),\qquad \mathcal{B}(\varphi,\tilde{\varphi})=\langle b,\tilde{\varphi}\rangle_{\partial\Omega}$$

$$\text{with}\quad \mathcal{B}(\varphi,\tilde{\varphi})=\int_{\partial\Omega}\int_{\partial\Omega}\varphi(\boldsymbol{\xi})G(\mathbf{x},\boldsymbol{\xi})\tilde{\varphi}(\mathbf{x})\,\mathrm{d}S_\xi\,\mathrm{d}S_x$$

- Leads to linear system of equations

$$\boxed{\mathbf{A}\boldsymbol{\varphi}=\mathbf{b}}\qquad (\mathbf{A}\in\mathbb{R}^{N\times N},\ \mathbf{b}\in\mathbb{R}^N)$$

where

$$A_{PQ}=\sum_{e'\in I(P)}\sum_{e\in I(Q)}\int_{\Delta_{e'}}N_P(\mathbf{a}')\Big\{\int_{\Delta_e}G(\mathbf{x}(\mathbf{a}'),\boldsymbol{\xi}(\mathbf{a}))N_Q(\mathbf{a})J(\mathbf{a})\,\mathrm{d}\mathbf{a}\Big\}J(\mathbf{a}')\,\mathrm{d}\mathbf{a}'$$

$$b_P=\sum_{e'\in I(P)}\int_{\Delta_{e'}}N_P(\mathbf{a}')b(\mathbf{x}(\mathbf{a}'))J(\mathbf{a}')\,\mathrm{d}\mathbf{a}'$$

- Matrix **A square, fully-populated, invertible, symmetric**

Limitations of “traditional” BEM

CPU for the main steps of traditional BEMs:

(a) Set-up of $\mathbf{A}$: CPU $= O(N^2)$;

(b) Solution using direct solver (usually LU factorization): CPU $= (N^3)$;

(c) Evaluation of integral representations at M points: CPU $= O(N \times M)$.

Besides:

(d) $O(N^2)$ memory needed for storing $\mathbf{A}$.
$\Longrightarrow$ Problem size N at most $O(10^4)$

Reasons fors (a)-(d):

- $G(\mathbf{x}, \boldsymbol{\xi})$ non-zero for all $(\mathbf{x}, \boldsymbol{\xi})$;
- Element matrices $\mathbf{A}^e(\mathbf{x}^P)$ recomputed for each new collocation point $\mathbf{x}^P$.

Overcoming the limitations of "traditional" BEM

Two issues:

1. To accelerate the BEM (i.e. to reduce its $O(N^3)$ **complexity**)
2. To increase permitted problem sizes.

Main ideas:

(i) Iterative solution of BEM matrix equation
$\Longrightarrow$ CPU $= O(N^2 \times N_I)$, with usually $N_I/N \to 0$;

(ii) Acceleration of matrix-vector product $\mathbf{A}\varphi$ for given density φ.
$\Longrightarrow$ complexity lower than $O(N^2)$.

Several strategies available for developing fast BEMs
The Fast Multipole Method (FMM) is the most developed to date.

The GMRES algorithm

- Linear system

$$\mathbf{Au} = \mathbf{b} \qquad \begin{cases} \mathbf{A} \in \mathbb{R}^{N\times N} \text{ or } \mathbb{C}^{N\times N}, \quad \mathbf{A} \text{ invertible} \\ \mathbf{u} \in \mathbb{R}^{N} \text{ ou } \mathbb{C}^{N}, \\ \mathbf{b} \in \mathbb{R}^{N} \text{ ou } \mathbb{C}^{N} \end{cases}$$

- Generalized Minimal RESiduals (GMRES): principle

$$\mathbf{u}^{(k)} = \underset{u\in u^{(0)}+V_k}{\arg\min} \, \|\mathbf{b}-\mathbf{Au}\|^2, \qquad V_k = \text{Vect}\{\mathbf{v}_1,\ldots,\mathbf{v}_k\} \text{ to be specified}$$

Explicit form of minimisation:

$$\mathbf{u}^{(k)} = \mathbf{u}^{(0)} + \sum_{j=1}^{k} \alpha_j^{(k)}\mathbf{v}_j$$

$$\text{with} \quad \boldsymbol{\alpha}^{(k)} \equiv (\alpha_1^{(k)},\ldots,\alpha_k^{(k)}) = \underset{\alpha_1,\ldots,\alpha_k}{\arg\min} \, \Big\| \mathbf{r}^{(0)} - \sum_{j=1}^{k} \alpha_j \, \mathbf{Av}_j \Big\|^2$$

- Iteration k: basis $(\mathbf{v}_1,\ldots,\mathbf{v}_{k-1})$ augmented with a new vector $\mathbf{v}_k$, hence $V_{k-1} \subset V_k$.

Minimization problem size increases with k: **restart** when $k > m$, GMRES(m)

The GMRES algorithm

- If $k = N$, one must have $\mathbf{u}^{(N)} = \mathbf{u}$ (hence convergence within $\leq N$ iterations
- In practice: (i) $N_{\text{iter}} \ll N$ is desired, (ii) exact convergence not necessary.

$$r^{(k)} \equiv \|\mathbf{b} - \mathbf{A}\mathbf{u}^{(k)}\| \leq \epsilon r^{(0)} \qquad (\epsilon\text{: } \textbf{tolerance})$$

- Construction of subspace $V_k = \text{Vect}\{\mathbf{v}_1, \ldots, \mathbf{v}_k\}$ using *Krylov vectors:*

$$V_k = \text{Vect}\{\, \mathbf{w}_1,\ \mathbf{w}_2 = \mathbf{A}\mathbf{w}_1,\ \ldots,\ \mathbf{w}_k = \mathbf{A}\mathbf{w}_{k-1} \,\} \qquad \text{with } \mathbf{w}_1 = \mathbf{r}^{(0)}$$

- Sequence $(\mathbf{v}_1, \ldots, \mathbf{v}_k)$ constructed using **orthonormalization** of Krylov vectors $(\mathbf{w}_1, \ldots, \mathbf{w}_k)$:

$$\begin{aligned} &\mathbf{v}_\ell^{\mathsf{T}}\mathbf{v}_k = 0 \\ &\|\mathbf{v}_k\| = 1 && \text{for all } k \geq 1 \\ &\text{Vect}\{\mathbf{w}_1, \ldots, \mathbf{w}_k\} = \text{Vect}\{\mathbf{v}_1, \ldots, \mathbf{v}_k\} = V_k \end{aligned}$$

Main contribution to computational cost: evaluation of matrix-vector products Aw for given w.

Preconditioning

- *Left preconditioning*:
$$\mathbf{M}^{-1}\mathbf{A}\mathbf{u} = \mathbf{M}^{-1}\mathbf{b}$$
Improved convergence (i.e. less iterations) if $\mathbf{M}^{-1}\mathbf{A}$ better conditioned than $\mathbf{A}$
- Krylov sequence associated with matrix $\mathbf{M}^{-1}\mathbf{A}$:
$$\mathbf{r}^{(0)} = \mathbf{M}^{-1}\mathbf{b} - \mathbf{M}^{-1}\mathbf{A}\mathbf{u}^{(0)} = \mathbf{w}_1 \qquad \text{i.e.} \quad \mathbf{M}\mathbf{w}_1 = \mathbf{b} - \mathbf{A}\mathbf{u}^{(0)}$$
$$\mathbf{w}_{k+1} = \mathbf{M}^{-1}\mathbf{A}\mathbf{w}_k \qquad \text{i.e.} \quad \mathbf{M}\mathbf{w}_{k+1} = \mathbf{A}\mathbf{w}_k \qquad (k \geq 0)$$
- Modified convergence criterion:
$$\|\mathbf{M}^{-1}\mathbf{b} - \mathbf{M}^{-1}\mathbf{A}\mathbf{u}^{(k)}\| \leq \epsilon \|\mathbf{M}^{-1}\mathbf{b}\|$$
- Many approaches available for definir preconditioning matrices $\mathbf{M}$:
  - → Diagonal preconditioneur $M_{ij} = A_{ij}\delta_{ij}$;
  - → Incomplete LU factorization of $\mathbf{A}$;
  - → Sparse approximate inverses;
  - → Multigrid approaches;
  - → Preconditioners exploiting specific features of the problems, e.g. single-inclusion case for many-inclusion problems.

Origins of the FMM: fast computation of potentials

$$\Phi(\mathbf{x}_i) = C \sum_{j=1}^{N_\xi} \frac{q_j}{\|\boldsymbol{\xi}_j - \mathbf{x}_i\|} \quad (1 \leq i \leq N_x)$$

$C = (4\pi\varepsilon_0)^{-1}$, electric charges q_j (electrostatic); $C = \mathcal{G}$, masses q_j (gravitation)

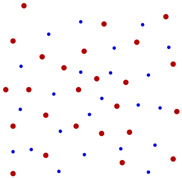

- Straightforward computation: $\text{CPU} = O(N_x N_\xi)$;
- Reason: influence coefficient $\|\boldsymbol{\xi}_j - \mathbf{x}_i\|^{-1}$ depends on both $\mathbf{x}_i$ and $\boldsymbol{\xi}_j$;
- **Fast summation** (Greengard, 1985): $\text{CPU} = O(N_x + N_\xi)$

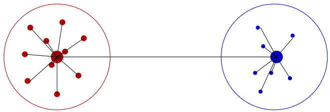

Iterative solution of integral equation

Model problem:

find φ, $\displaystyle\int_{\partial\Omega} G(\mathbf{x},\boldsymbol{\xi})\varphi(\boldsymbol{\xi})\,\mathrm{d}S_\xi = b(\mathbf{x})$, i.e. $\boxed{\mathcal{S}[\varphi,\partial\Omega](\mathbf{x}) = b(\mathbf{x}) \quad (\mathbf{x}\in\partial\Omega)}$

Krylov vector: $\mathbf{A}\boldsymbol{\varphi}$ discretized version of

$$\mathcal{S}[\varphi,\partial\Omega](\mathbf{x}) := \int_{\partial\Omega} G(\mathbf{x},\boldsymbol{\xi})\varphi(\boldsymbol{\xi})\,\mathrm{d}S_\xi$$

Integral operator $\mathcal{S}$: a generalization to infinite-dimensional function spaces (here $H^{-1/2}(\partial\Omega)$) of the concept of matrix.

- Using traditional BEM: $\text{CPU} = O(N^2)$ for each evaluation of $\mathbf{A}\boldsymbol{\varphi}$;
- **Aim of the Fast Multipole Method:** evaluation of $\mathbf{A}\boldsymbol{\varphi}$ at CPU cost **lower than $O(N^2)$.**

FMM: main ideas

$$\mathcal{S}[\varphi,\partial\Omega](\mathbf{x}) := \int_{\partial\Omega} G(\mathbf{x},\boldsymbol{\xi})\varphi(\boldsymbol{\xi})\,\mathrm{d}S_{\xi}$$

- **Main idea:** seek to **reuse** element integrations (w.r.t. $\boldsymbol{\xi}$) when collocation point $\mathbf{x}$ is changed;
- **Method:** express the fundamental solution as a **series of products:**

$$G(\mathbf{x},\boldsymbol{\xi}) = \sum_{n=0}^{\infty} g_n(\mathbf{x})h_n(\boldsymbol{\xi})$$

  and truncate the series at suitable level p:

$$G(\mathbf{x},\boldsymbol{\xi}) = \sum_{n=0}^{p} g_n(\mathbf{x})h_n(\boldsymbol{\xi}) + \epsilon_G(p)$$

- **Consequence:**

$$\mathcal{S}[\varphi,\partial\Omega](\mathbf{x}) = \sum_{n=0}^{p} g_n(\mathbf{x}) \int_{\partial\Omega} h_n(\boldsymbol{\xi})\varphi(\boldsymbol{\xi})\,\mathrm{d}S_{\xi} + \epsilon(p)$$

  The p integrations are independent on $\mathbf{x}$ and are reusable as $\mathbf{x}$ is changed.

FMM: main ideas

How to express $G(\mathbf{x}, \xi)$ as a sum (series) of products? Taylor expansion about origins $\mathbf{x}_0$ and $\boldsymbol{\xi}_0$:

$$G(\mathbf{x},\xi) = \sum_{m\geq 0} \frac{1}{m!}[\partial_\xi^m G](\mathbf{x},\boldsymbol{\xi}_0)\,(\xi-\boldsymbol{\xi}_0)^m$$

$$= \sum_{n\geq 0}\sum_{m\geq 0} \frac{1}{m!n!}[\partial_x^n\partial_\xi^m G](\mathbf{x}_0,\boldsymbol{\xi}_0)\,(\mathbf{x}-\mathbf{x}_0)^n(\xi-\boldsymbol{\xi}_0)^m$$

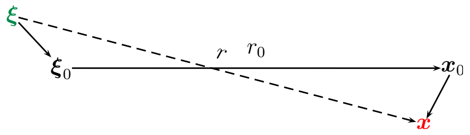

For Laplace kernel $1/r$: sophisticated version of Taylor expansion leads to **multipole expansion** (see next).

Multipole expansion of $1/r$

The Multipole expansion of $1/r$ is given (see proof later) by:

$$\frac{1}{\|\boldsymbol{\xi}-\mathbf{x}\|} = \sum_{n=0}^{+\infty}\sum_{m=-n}^{n} R_{n,m}(\mathbf{x}-\mathbf{x}_0)\sum_{n'=0}^{+\infty}\sum_{m'=-n'}^{n'}(-1)^n\overline{S_{n+n',m+m'}(\boldsymbol{\xi}_0-\mathbf{x}_0)}R_{n',m'}(\boldsymbol{\xi}-\boldsymbol{\xi}_0)$$

$$R_{n,m}(\mathbf{z}) = \frac{1}{(n+m)!}P_n^m(\cos\alpha)e^{\mathrm{i}m\beta}\rho^n$$

$$S_{n,m}(\mathbf{z}) = (n-m)!P_n^m(\cos\alpha)e^{\mathrm{i}m\beta}\frac{1}{\rho^{n+1}}$$

$$\text{with } \mathbf{z} = \rho\big[\sin\alpha(\cos\beta\,\mathbf{e}_1+\sin\beta\,\mathbf{e}_2)\big)+\cos\alpha\,\mathbf{e}_3\big]$$

Conditions for convergence of the multipole expansion:

$$\|\mathbf{x}-\mathbf{x}_0\| < \|\boldsymbol{\xi}-\mathbf{x}_0\| \quad \text{and} \quad \|\boldsymbol{\xi}-\boldsymbol{\xi}_0\| < \|\mathbf{x}-\boldsymbol{\xi}_0\|$$

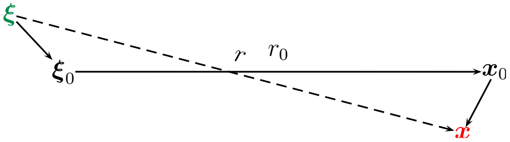

Multipole expansion of $1/r$: computation of solid harmonics $R_{n,m}$, $S_{n,m}$

Solid harmonics $R_{n,m}$ and $S_{n,m}$ evaluated **using Cartesian coordinates** using recursion formulae derived from those for Legendre polynomials:

- The $R_{n,m}(\mathbf{z})$ are computed recursively by setting $R_{0,0}(\mathbf{z}) = 1$ and using

$$R_{n+1,n+1}(\mathbf{z}) = \frac{z_1 + \mathrm{i}z_2}{2(n+1)} R_{n,n}(\mathbf{z})$$

$$((n+1)^2 - m^2)R_{n+1,m}(\mathbf{z}) - (2n+1)z_3 R_{n,m}(\mathbf{z}) + |\mathbf{z}|^2 R_{n-1,m}(\mathbf{z}) = 0 \quad (n \geq m)$$

- The $S_{n,m}(\mathbf{z})$ are computed recursively by setting $S_{0,0}(\mathbf{z}) = 1/|\mathbf{z}|$ and using

$$S_{n+1,n+1}(\mathbf{z}) = \frac{(2n+1)(z_1 + \mathrm{i}z_2)}{|\mathbf{z}|^2} R_{n,n}(\mathbf{z})$$

$$|\mathbf{z}|^2 S_{n+1,m}(\mathbf{z}) - (2n+1)z_3 S_{n,m}(\mathbf{z}) + (n^2 - m^2)S_{n-1,m}(\mathbf{z}) = 0 \quad (n \geq m)$$

- Finally, $R_{n,m}(\mathbf{z})$ and $S_{n,m}(\mathbf{z})$ for negative values of m are computed via the identities

$$R_{n,-m}(\mathbf{z}) = (-1)^m \overline{R_{n,m}(\mathbf{z})} \qquad S_{n,-m}(\mathbf{z}) = (-1)^m \overline{S_{n,m}(\mathbf{z})}$$

Multipole expansion of $1/r$: computation of solid harmonics $R_{n,m}$, $S_{n,m}$

Derivatives of the $R_{n,m}$:

$$\frac{\partial}{\partial z_1} R_{n,m}(\mathbf{z}) = \frac{1}{2}(R_{n-1,m-1} - R_{n-1,m+1})(\mathbf{z})$$

$$\frac{\partial}{\partial z_2} R_{n,m}(\mathbf{z}) = \frac{i}{2}(R_{n-1,m-1} + R_{n-1,m+1})(\mathbf{z})$$

$$\frac{\partial}{\partial z_3} R_{n,m}(\mathbf{z}) = R_{n-1,m}$$

Multipole expansion of $1/r$: proof (1/4)

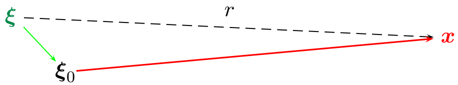

$$G(\mathbf{x},\boldsymbol{\xi}) = \frac{1}{4\pi\|\boldsymbol{\xi}-\mathbf{x}\|}$$

$$\boldsymbol{\xi}-\mathbf{x} = (\boldsymbol{\xi}-\boldsymbol{\xi}_0) - (\mathbf{x}-\boldsymbol{\xi}_0)$$

Spherical coordinates:

$$(\boldsymbol{\xi}-\boldsymbol{\xi}_0) = \rho\big[\sin\alpha(\cos\beta\,\mathbf{e}_1 + \sin\beta\,\mathbf{e}_2) + \cos\alpha\,\mathbf{e}_3\big]$$

$$(\mathbf{x}-\boldsymbol{\xi}_0) = R\big[\sin\theta(\cos\varphi\,\mathbf{e}_1 + \sin\varphi\,\mathbf{e}_2) + \cos\theta\,\mathbf{e}_3\big]$$

$$\boxed{\frac{1}{\|\boldsymbol{\xi}-\mathbf{x}\|} = (R^2 - 2\rho R\cos\Phi + \rho^2)^{-1/2}}$$

$$\cos\Phi = \frac{1}{\rho R}(\boldsymbol{\xi}-\boldsymbol{\xi}_0)\cdot(\mathbf{x}-\boldsymbol{\xi}_0) = \sin\alpha\sin\theta\cos(\beta-\varphi) + \cos\alpha\cos\theta$$

Multipole expansion of $1/r$: proof (2/4)

$$\frac{1}{\|\boldsymbol{\xi}-\mathbf{x}\|} = (R^2 - 2\rho R\cos\Phi + \rho^2)^{-1/2}$$
$$= \frac{1}{R}(1 - 2zt + t^2)^{-1/2} \qquad \Big(z = \cos\Phi, \quad t = \frac{\rho}{R} \Big)$$

Since $(1-2zt+t^2)^{-1/2}$ is the generating function of the Legendre polynomials, i.e.:

$$(1 - 2zt + t^2)^{-1/2} = \sum_{n\geq 0} P_n(z)t^n \qquad (t < 1)$$

one has:

$$\boxed{\frac{1}{\|\boldsymbol{\xi}-\mathbf{x}\|} = \sum_{n=0}^{+\infty} \frac{P_n(\cos\Phi)}{R^{n+1}}\rho^n} \qquad (\rho < R)$$

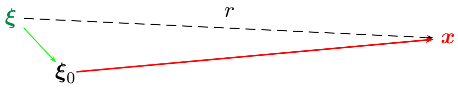

Multipole expansion of $1/r$: proof (3/4)

$$\boxed{\frac{1}{\|\boldsymbol{\xi}-\mathbf{x}\|} = \sum_{n=0}^{+\infty} \frac{P_n(\cos\Phi)}{R^{n+1}}\rho^n} \qquad (\rho < R)$$

To recast as a series of products $g(\rho,\alpha,\beta)h(R,\theta,\varphi)$: addition theorem for Legendre polynomials:

$$P_n(\cos\Phi) = \sum_{m=-n}^{n} \frac{(n-m)!}{(n+m)!}\Big(P_n^m(\cos\alpha)e^{\mathrm{i}m\beta}\Big)\Big(P_n^m(\cos\theta)e^{-\mathrm{i}m\varphi}\Big)$$

$$\boxed{\frac{1}{\|\boldsymbol{\xi}-\mathbf{x}\|} = \sum_{n=0}^{+\infty}\sum_{m=-n}^{n} R_{n,m}(\boldsymbol{\xi}-\boldsymbol{\xi}_0)\overline{S_{n,m}(\mathbf{x}-\boldsymbol{\xi}_0)}}$$

$$R_{n,m}(\mathbf{z}) = \frac{1}{(n+m)!}P_n^m(\cos\alpha)e^{\mathrm{i}m\beta}\rho^n$$

$$S_{n,m}(\mathbf{z}) = (n-m)!P_n^m(\cos\theta)e^{\mathrm{i}m\varphi}\frac{1}{R^{n+1}}$$

The series is convergent if $\|\boldsymbol{\xi}-\boldsymbol{\xi}_0\| < \|\mathbf{x}-\boldsymbol{\xi}_0\|$.

Multipole expansion of $1/r$: proof (4/4)

$$\frac{1}{\|\xi - \mathbf{x}\|} = \sum_{n=0}^{+\infty} \sum_{m=-n}^{n} R_{n,m}(\xi - \xi_0)\overline{S_{n,m}(\mathbf{x} - \xi_0)}$$

Application to evaluation of potentials:

$$\Phi(\mathbf{x}_i) = C \sum_{j=1}^{N_\xi} \frac{q_j}{\|\xi_j - \mathbf{x}_i\|} = C \sum_{n=0}^{+\infty} \sum_{m=-n}^{n} M_{n,m}(\xi_0)\overline{S_{n,m}(\mathbf{x}_i - \xi_0)}\Big\}$$

with **multipole moments** defined by

$$M_{n,m}(\xi_0) = \sum_{j=1}^{N_\xi} q_j R_{n,m}(\xi_j - \xi_0)$$

Truncation of series to $n < p$ (with error control available, see later):

- Evaluation of $N_\xi N_x$ influence coefficients $\|\xi_j - \mathbf{x}_i\|^{-1}$ replaced with evaluation of $p^2 N_x$ products $M_{n,m}(\xi_0)\overline{S_{n,m}(\mathbf{x}_i - \xi_0)}$

Multipole expansion of $1/r$: proof

Insertion of local origin $\mathbf{x}_0$ into $\mathbf{x}_i - \boldsymbol{\xi}_0$:

- Note identity

$$S_{n,m}(\mathbf{z}) = (-1)^n \Big(\frac{\partial}{\partial z_1} + \mathrm{i} \frac{\partial}{\partial z_2} \Big)^m \frac{\partial^{n-m}}{\partial z_3^{n-m}} \frac{1}{\|\mathbf{z}\|} \qquad (m > 0) \qquad \text{(a)}$$

$$= (-1)^{n+m} \Big(\frac{\partial}{\partial z_1} - \mathrm{i} \frac{\partial}{\partial z_2} \Big)^{-m} \frac{\partial^{n+m}}{\partial z_3^{n+m}} \frac{1}{\|\mathbf{z}\|} \qquad (m < 0) \qquad \text{(b)}$$

- Invoke multipole expansion of $1/\|\mathbf{z}\|$ with $\mathbf{z} = (\mathbf{x}_i - \mathbf{x}_0) - (\boldsymbol{\xi}_0 - \mathbf{x}_0)$:

$$\frac{1}{\|\mathbf{x}_i - \boldsymbol{\xi}_0\|} = \sum_{n'=0}^{+\infty} \sum_{m'=-n'}^{n} R_{n',m'}(\mathbf{x}_i - \mathbf{x}_0) \overline{S_{n',m'}(\boldsymbol{\xi}_0 - \mathbf{x}_0)}$$

- Use representation (a,b) for $S_{n',m'}(\boldsymbol{\xi}_0 - \mathbf{x}_0)$;
- Exploit harmonicity of $1/\|\boldsymbol{\xi}_0 - \mathbf{x}_0\|$ via

$$\Big(\frac{\partial}{\partial \xi_1^0} + \mathrm{i} \frac{\partial}{\partial \xi_2^0} \Big) \Big(\frac{\partial}{\partial \xi_1^0} - \mathrm{i} \frac{\partial}{\partial \xi_2^0} \Big) \frac{1}{\|\boldsymbol{\xi}_0 - \mathbf{x}_0\|} + \frac{\partial^2}{\partial {\xi_3^0}^2} \frac{1}{\|\boldsymbol{\xi}_0 - \mathbf{x}_0\|} = 0$$

- Reorder and reorganize resulting formula

$$\boxed{S_{n,m}(\mathbf{x}_i - \boldsymbol{\xi}_0) = \sum_{n'=0}^{+\infty} \sum_{m'=-n'}^{n} \overline{R_{n',m'}(\mathbf{x}_i - \mathbf{x}_0)} S_{n+n',m+m'}(\boldsymbol{\xi}_0 - \mathbf{x}_0)}$$

Multipole expansion: truncation error

Assume one can find $R > 0$ and $\chi > 1$ such that

$$\big(\|\mathbf{x}-\mathbf{x}_0\| < R \text{ et } \|\boldsymbol{\xi}-\mathbf{x}_0\| > \chi R\big) \quad \text{et} \quad \big(\|\boldsymbol{\xi}-\boldsymbol{\xi}_0\| < R \text{ et } \|\mathbf{x}-\boldsymbol{\xi}_0\| > \chi R\big)$$

An upper bound of the error arising from truncating the multipole expansion at order p is:

$$\Big| \frac{1}{\|\boldsymbol{\xi}-\mathbf{x}\|} - \sum_{n=0}^{p} \sum_{m=-n}^{n} R_{n,m}(\mathbf{x}-\mathbf{x}_0) \sum_{n'=0}^{p} \sum_{m'=-n'}^{n'} (-1)^n \overline{S_{n+n',m+m'}(\boldsymbol{\xi}_0-\mathbf{x}_0)} R_{n',m'}(\boldsymbol{\xi}-\boldsymbol{\xi}_0) \Big| \leq \frac{1}{R(\chi-1)\chi^{p+1}}$$

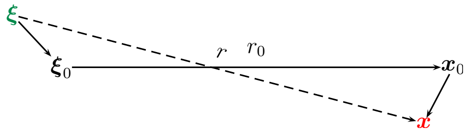

The truncation error is scale-independent

Single-level fast multipole method

Boundary of interest enclosed in a cubic grid

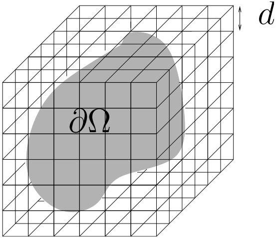

Convergence of multipole expansion guaranteed if **x** and $\boldsymbol{\xi}$ lie in non-adjacent cells, with

$$\chi \geq \sqrt{3}$$

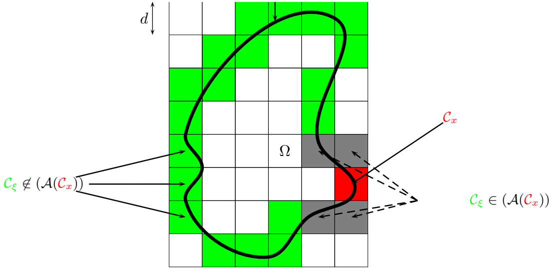

Single-level FMM

- Matrix-vector product $\longleftarrow$ integral operator evaluation

$$\mathcal{S}[\varphi,\partial\Omega](\mathbf{x}) = \int_{\partial\Omega} G(\mathbf{x},\boldsymbol{\xi})\varphi(\boldsymbol{\xi})\,\mathrm{d}S_\xi$$

- Split into **near** and **far** contributions:

$$\int_{\partial\Omega} = \sum_{\mathcal{C}_\xi\in\mathcal{A}(\mathcal{C}_x)} \int_{\partial\Omega\cap\mathcal{C}_\xi} + \sum_{\mathcal{C}_\xi\notin\mathcal{A}(\mathcal{C}_x)} \int_{\partial\Omega\cap\mathcal{C}_\xi}$$

$$\mathcal{S}[\varphi,\partial\Omega](\mathbf{x}) = \mathcal{S}[\varphi,\partial\Omega]^{\text{near}}(\mathbf{x}) + \mathcal{S}[\varphi,\partial\Omega]^{\text{far}}(\mathbf{x})$$

Single-level FMM

Far contribution $\mathcal{S}[\varphi,\partial\Omega]^{\text{far}}(\mathbf{x})$:

$$\mathcal{S}[\varphi,\partial\Omega]^{\text{far}}(\mathbf{x}) = \sum_{\mathcal{C}_\xi \notin \mathcal{A}(\mathcal{C}_x)} \int_{\partial\Omega\cap\mathcal{C}_\xi} G(\mathbf{x},\boldsymbol{\xi})\varphi(\boldsymbol{\xi})\,\mathrm{d}S_\xi \qquad (\mathbf{x}\in\mathcal{C}_x)$$

Introduce (truncated) multipole expansion of $G(\mathbf{x},\boldsymbol{\xi})$, with $\boldsymbol{\xi}_0$ and $\mathbf{x}_0$ chosen as centres of cells $\mathcal{C}_\xi$ and $\mathcal{C}_x$:

$$\mathcal{S}[\varphi,\partial\Omega]^{\text{far}}(\mathbf{x}) \approx \sum_{\mathcal{C}_\xi \notin \mathcal{A}(\mathcal{C}_x)} \frac{1}{4\pi} \sum_{n=0}^{p}\sum_{m=-n}^{n} R_{n,m}(\mathbf{x}-\mathbf{x}_0) \sum_{n'=0}^{p}\sum_{m'=-n'}^{n'} (-1)^n \overline{S_{n+n',m+m'}(\boldsymbol{\xi}_0-\mathbf{x}_0}$$

$$\times \int_{\partial\Omega\cap\mathcal{C}_\xi} R_{n',m'}(\boldsymbol{\xi}-\boldsymbol{\xi}_0)\varphi(\boldsymbol{\xi})\,\mathrm{d}S_\xi$$

$$= \frac{1}{4\pi} \sum_{n=0}^{p}\sum_{m=-n}^{n} R_{n,m}(\mathbf{x}-\mathbf{x}_0)$$

$$\sum_{\mathcal{C}_\xi \notin \mathcal{A}(\mathcal{C}_x)} \sum_{n'=0}^{p}\sum_{m'=-n'}^{n'} (-1)^n \overline{S_{n+n',m+m'}(\boldsymbol{\xi}_0-\mathbf{x}_0)}\, M_{n',m'}(\mathcal{C}_\xi)$$

$p \quad n$

Single-level FMM

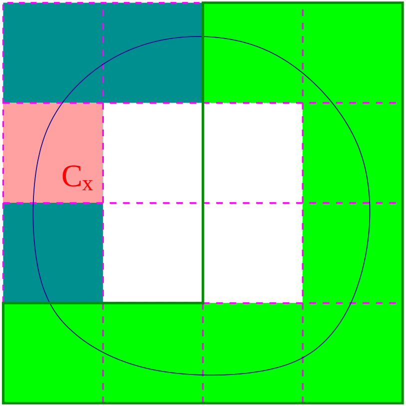

Single-level FMM: complexity

1. Compute and store multipole moments $M_{n,m}(\mathcal{C}_\xi)$ for each integration cell:
   $\text{CPU} = O(p^2 \times N_\text{B} \times (N/N_\text{B})) = O(p^2 \times N)$.
2. For each collocation cell $\mathcal{C}_x$:
   (a) Compute local coefficients $L_{n,m}(\mathcal{C}_x, \mathcal{C}_\xi)$ (M2L):
   $\text{CPU} = O(p^2 \times p^2 \times N_\text{B}) = O(p^4 \times N_\text{B})$;

$$L_{n,m}(\mathcal{C}_x) = \sum_{\mathcal{C}_\xi \notin \mathcal{A}(\mathcal{C}_x)} \sum_{n'=0}^{p} \sum_{m'=-n'}^{n'} (-1)^n \overline{S_{n+n',m+m'}(\boldsymbol{\xi}_0 - \mathbf{x}_0)}\, M_{n',m'}(\mathcal{C}_\xi)$$

   (b) Far contribution $\mathcal{S}[\varphi, \partial\Omega]^{\text{far}}(\mathbf{x})$ to integral operator, for all $\mathbf{x} \in \mathcal{C}_x$:
   $\text{CPU} = O(p^2 \times (N/N_\text{B}))$

$$\mathcal{S}[\varphi, \partial\Omega]^{\text{far}}(\mathbf{x}) = \sum_{n=0}^{+\infty} \sum_{m=-n}^{n} R_{n,m}(\mathbf{x} - \mathbf{x}_0) L_{n,m}(\mathcal{C}_x)$$

   (c) Near contribution $\mathcal{S}[\varphi, \partial\Omega]^{\text{near}}(\mathbf{x})$ to integral operator, using standard BEM procedures: $\text{CPU} = O\big(\,|\mathcal{A}(\mathcal{C}_x)| \times (N/N_\text{B}) \times (N/N_\text{B})\,\big) = O(|\mathcal{A}\big(\,\mathcal{C}_x)| \times N^2/N_\text{B}^2\,\big)$

Single-level FMM: optimal complexity

Total CPU time for one evaluation of $\mathcal{S}[\varphi, \partial\Omega]$:

$$\begin{aligned} \text{CPU} &= Ap^2N + N_{\text{B}}\Big(Bp^4N_{\text{B}} + Cp^2(N/N_{\text{B}}) + D\,|\mathcal{A}(\mathcal{C}_x)|\,N^2/N_{\text{B}}^2\Big) \\ &= (A+C)p^2N + Bp^4N_{\text{B}}^2 + DN^2/N_{\text{B}} \end{aligned}$$

Optimal choice: $N_{\text{B}} = O(N^{2/3})$, yielding CPU / GMRES iteration $= O(N^{4/3})$

- Single-level FMM (Laplace and other elliptic PDEs): $\text{CPU} = O(N^{4/3})$;
- To further improve complexity: **multi-level FMM**

Multi-level FMM

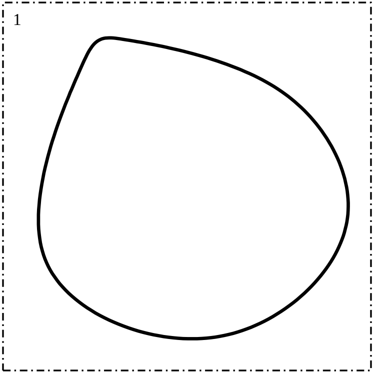

Multi-level FMM: initialization of multipole moments

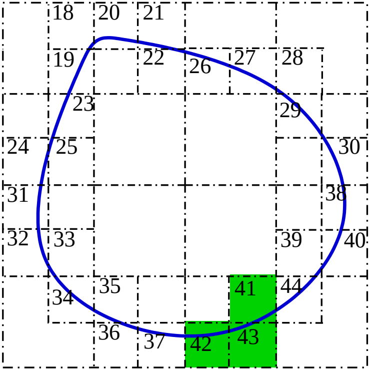

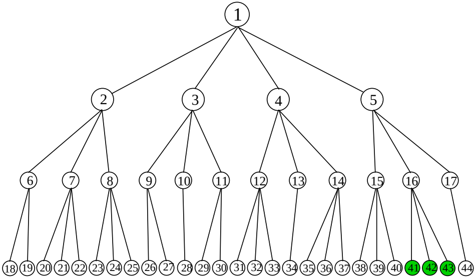

Computation of multipole moments, leaf level cells ($\ell = \bar{\ell} = 3$ here):

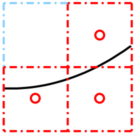

$$M_{n,m}(\mathcal{C}_{\xi}^{(\bar{\ell})}; \boldsymbol{\xi}_0^{(\bar{\ell})}) = \int_{\partial\Omega \cap \mathcal{C}_{\xi}^{(\bar{\ell})}} R_{n,m}(\boldsymbol{\xi} - \boldsymbol{\xi}_0^{(\bar{\ell})}) \varphi(\boldsymbol{\xi}) \, \mathrm{d}S_{\xi}$$

Multi-level FMM: upward pass

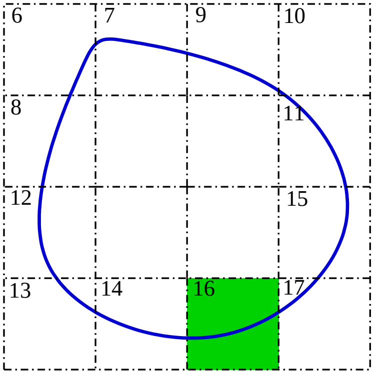

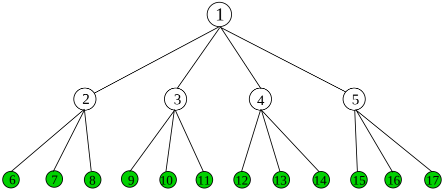

Computation of multipole moments, parent cells ($\ell = 3 \to \ell = 2$ here):

$$M_{n,m}(\mathcal{C}_\xi^{(\ell-1)}; \boldsymbol{\xi}_0^{(\ell-1)}) = \sum_{\mathcal{C}_\xi^{(\ell)} \in \text{Children}(\mathcal{C}_\xi^{(\ell-1)})} M_{n,m}(\mathcal{C}_\xi^{(\ell)}; \boldsymbol{\xi}_0^{(\ell-1)}) \qquad \text{(M2M)}$$

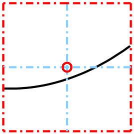

Upward pass needs translation of origin $\boldsymbol{\xi}_0^{(\ell)} \to \boldsymbol{\xi}_0^{(\ell-1)}$ in $M_{n,m}(\mathcal{C}_\xi^{(\ell)}; \boldsymbol{\xi}_0^{(\ell)})$

Multi-level FMM: M2M translation formula for upward pass

$$M_{n,m}(\mathcal{C}_\xi^{(\ell-1)};\boldsymbol{\xi}_0^{(\ell-1)}) = \sum_{\mathcal{C}_\xi^{(\ell)}\in\text{Children}(\mathcal{C}_\xi^{(\ell-1)})} \int_{\partial\Omega\cap\mathcal{C}_\xi^{(\bar{\ell})}} R_{n,m}(\boldsymbol{\xi}-\boldsymbol{\xi}_0^{(\ell-1)})\varphi(\boldsymbol{\xi})\,\mathrm{d}S_\xi$$

M2M translation identity:

$$R_{n,m}(\boldsymbol{\xi}-\boldsymbol{\xi}_0^{(\ell-1)}) = \sum_{n'=0}^{\infty}\sum_{m'=-n'}^{n'} R_{n',m'}(\boldsymbol{\xi}_0^{(\ell)}-\boldsymbol{\xi}_0^{(\ell-1)})R_{n-n',m-m'}(\boldsymbol{\xi}-\boldsymbol{\xi}_0^{(\ell)})$$

$$M_{n,m}(\mathcal{C}_\xi^{(\ell)};\boldsymbol{\xi}_0^{(\ell-1)}) = \sum_{n'=0}^{\infty}\sum_{m'=-n'}^{n'} R_{n',m'}(\boldsymbol{\xi}_0^{(\ell)}-\boldsymbol{\xi}_0^{(\ell-1)})M_{n-n',m-m'}(\mathcal{C}_\xi^{(\ell)};\boldsymbol{\xi}_0^{(\ell)})$$

Multi-level FMM: M2M translation formula for upward pass

Proof:

- write $\|\mathbf{x}-\boldsymbol{\xi}\|^{-1}$ in two ways (inserting either $\boldsymbol{\xi}_0^{(\ell-1)}$ or $\boldsymbol{\xi}_0^{(\ell)}$ as pole):

$$\frac{1}{\|\mathbf{x}-\boldsymbol{\xi}\|} = \sum_{n=0}^{+\infty} \sum_{m=-n}^{n} R_{n,m}(\boldsymbol{\xi}-\boldsymbol{\xi}_0^{(\ell)})\overline{S_{n,m}(\mathbf{x}-\boldsymbol{\xi}_0^{(\ell)})} \qquad \text{(a)}$$

$$= \sum_{n=0}^{+\infty} \sum_{m=-n}^{n} R_{n,m}(\boldsymbol{\xi}-\boldsymbol{\xi}_0^{(\ell-1)})\overline{S_{n,m}(\mathbf{x}-\boldsymbol{\xi}_0^{(\ell-1)})} \qquad \text{(b)}$$

- Invoke identity

$$S_{n,m}(\mathbf{x}-\boldsymbol{\xi}_0^{(\ell-1)}) = (-1)^n \sum_{n'=0}^{+\infty} \sum_{m'=-n'}^{n} \overline{R_{n',m'}(\boldsymbol{\xi}_0^{(\ell-1)}-\boldsymbol{\xi}_0^{(\ell)})} S_{n+n',m+m'}(\mathbf{x}-\boldsymbol{\xi}_0^{(\ell)})$$

- Redefine summation indices $((n,m) \leftarrow (n+n',\ m+m'))$, reorder summations
- Identify cofactors of $S_{n,m}(\mathbf{x}-\boldsymbol{\xi}_0^{(\ell-1)})$ in (a) and (b)

$$\boxed{R_{n,m}(\boldsymbol{\xi}-\boldsymbol{\xi}_0^{(\ell-1)}) = \sum_{n'=0}^{\infty} \sum_{m'=-n'}^{n'} R_{n',m'}(\boldsymbol{\xi}_0^{(\ell)}-\boldsymbol{\xi}_0^{(\ell-1)}) R_{n-n',m-m'}(\boldsymbol{\xi}-\boldsymbol{\xi}_0^{(\ell)})}$$

Multi-level FMM: definition of interaction list

Definition of interaction list $\mathcal{I}(\mathcal{C})$:

$$\mathcal{C}' \in \mathcal{I}(\mathcal{C}) \Longleftrightarrow \mathcal{C}' \notin \mathcal{A}(\mathcal{C}) \text{ but } \mathsf{Father}(\mathcal{C}') \in \mathcal{A}(\mathsf{Father}(\mathcal{C}))$$

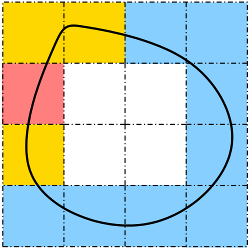

$\ell = 2$

$\mathcal{C}' \in \mathcal{I}(\mathcal{C})$

$\mathcal{C}'' \in \mathcal{A}(\mathcal{C})$

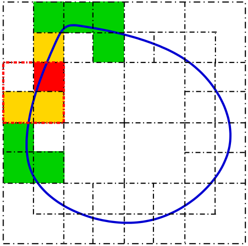

$\ell = 3$

Note: $\mathcal{C}' \in \mathcal{I}(\mathcal{C}) \Longleftrightarrow \mathcal{C}' \notin \mathcal{A}(\mathcal{C})$ for level $\ell = 2$.

Multi-level FMM: definition of interaction list

General case, for generic cell $\mathcal{C}$:

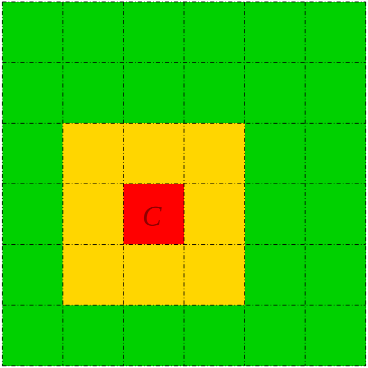

$\mathcal{C}' \in \mathcal{I}(\mathcal{C})$
$\mathcal{C}'' \in \mathcal{A}(\mathcal{C})$

$\mathcal{I}(\mathcal{C})$ contains up to

- $6^3 - 3^3 = 189$ cells (3-D);
- $6^2 - 3^2 = 27$ cells (2-D)

Multi-level FMM: M2L translation, upper level $\ell = 2$

M2L translation formula between **disjoint** same-level cells:

$$L_{n,m}(\mathcal{C}_x^{(\ell)}) = \sum_{\mathcal{C}_\xi \notin \mathcal{A}(\mathcal{C}_x^{(\ell)})} \sum_{n'=0}^{p} \sum_{m'=-n'}^{n'} (-1)^n \overline{S_{n+n',m+m'}(\boldsymbol{\xi}_0^{(\ell)} - \mathbf{x}_0^{(\ell)})} \, M_{n',m'}(\mathcal{C}_\xi^{(\ell)})$$

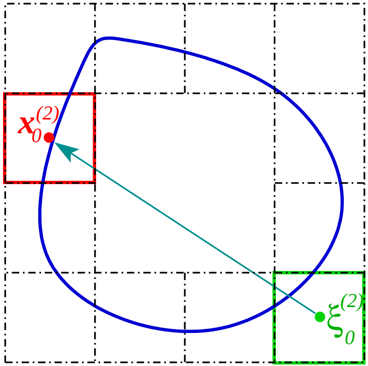

Multi-level FMM: M2L translation, upper level $\ell = 2$

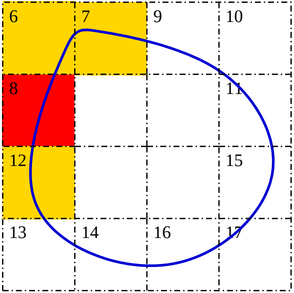

- Collocation cell $\mathcal{C}_x^{(0)}$: no action taken
- Collocation cell $\mathcal{C}_x^{(1)}$: no action taken
- Collocation cell $\mathcal{C}_x^{(2)}$: **initialize M2L**

$$L_{n,m}(\mathcal{C}_x^{(2)}) = \sum_{\mathcal{C}_\xi^{(2)} \notin \mathcal{A}(\mathcal{C}_x^{(2)})} \sum_{n'=0}^{p} \sum_{m'=-n'}^{n'} (-1)^n \overline{S_{n+n',m+m'}(\boldsymbol{\xi}_0^{(2)} - \mathbf{x}_0^{(2)})}\, M_{n',m'}(\mathcal{C}_\xi^{(2)})$$

To apply M2L to $\mathcal{A}(\mathcal{C}_x^{(2)})$: **subdivision**

Multi-level FMM: M2L translation, downward pass

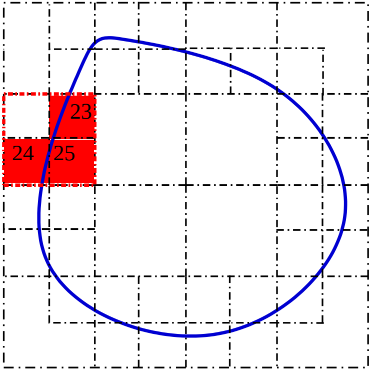

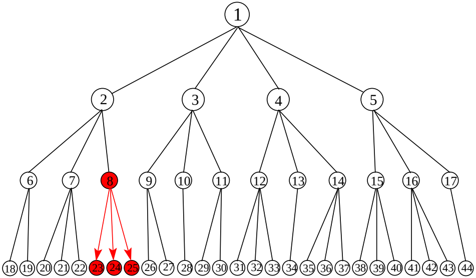

$$L_{n,m}(\mathcal{C}_x^{(\ell)};\mathbf{x}_0^{(\ell)}) = L_{n,m}(\mathcal{C}_x^{(\ell-1)};\mathbf{x}_0^{(\ell)}) + \sum_{\mathcal{C}_\xi^{(\ell)}\in\mathcal{I}(\mathcal{C}_x^{(\ell)})} \sum_{n'=0}^{p} \sum_{m'=-n'}^{n'} (-1)^n \overline{S_{n+n',m+m'}(\boldsymbol{\xi}_0^{(\ell)}-\mathbf{x}_0^{(\ell)})}\, M_{n',m'}(\mathcal{C}_\xi^{(\ell)})$$

Downward pass entails translation of origin $\mathbf{x}_0^{(\ell-1)} \to \mathbf{x}_0^{(\ell)}$

Multi-level FMM: M2L translation formula for downward pass

$$L_{n,m}(\mathcal{C}_x^{(\ell-1)};\mathbf{x}_0^{(\ell)}) = \sum_{n'=0}^{\infty}\sum_{m'=-n'}^{n'} R_{n'-n,m'-m}(\mathbf{x}_0^{(\ell)}-\mathbf{x}_0^{(\ell-1)})L_{n',m'}(\mathcal{C}_x^{(\ell-1)};\mathbf{x}_0^{(\ell-1)})$$

Proof: one must have

$$\sum_{n=0}^{\infty}\sum_{m=-n}^{n} R_{n,m}(\mathbf{x}-\mathbf{x}_0^{(\ell)})L_{n,m}(\mathcal{C}_x^{(\ell-1)};\mathbf{x}_0^{(\ell)}) \qquad \text{(a)}$$

$$= \sum_{n=0}^{\infty}\sum_{m=-n}^{n} R_{n,m}(\mathbf{x}-\mathbf{x}_0^{(\ell-1)})L_{n,m}(\mathcal{C}_x^{(\ell-1)};\mathbf{x}_0^{(\ell-1)}) \qquad \text{(b)}$$

Then, insert identity

$$R_{n,m}(\mathbf{x}-\mathbf{x}_0^{(\ell-1)}) = \sum_{n'=0}^{\infty}\sum_{m'=-n'}^{n'} R_{n',m'}(\mathbf{x}-\mathbf{x}_0^{(\ell)})R_{n-n',m-m'}(\mathbf{x}_0^{(\ell)}-\mathbf{x}_0^{(\ell-1)})$$

into (b) and identify cofactors of $R_{n,m}(\mathbf{x}-\mathbf{x}_0^{(\ell)})$ in (a) and (b)

Multi-level FMM: overall complexity

Fixed number M of DOFs per leaf cell

$\Longrightarrow \bar{\ell} = O(\log N)$ and $O(N/M)$ leaf cells;

Each non-empty level-ℓ cell has (on average) 4 non-empty children cells

$\Longrightarrow$ on average, $N^{(\ell)} = O(4^{-\ell}N)$ DOFs per level-ℓ cell

(i) Evaluation of multipole moments in leaf cells:

$$\text{CPU} = O(p^2 \times M \times (N/M)) = O(p^2 N)$$

(ii) Upward pass (M2M):

$$\text{CPU} = O(p^4 \times (N/M)[1 + 4^{-1} \ldots + 4^{3-\bar{\ell}}] = O(p^4 N/M)$$

(iii) Transfer (M2L) at each level $2 \leq \ell \leq \bar{\ell}$ from interaction list of each cell:

$$\text{CPU} = O(p^4 \times (N/M)[1 + 4^{-1} \ldots + 4^{2-\bar{\ell}}] = O(p^4 N/M);$$

(iv) Downward pass (L2L) at each level:

$$\text{CPU} = O(p^4 \times (N/M)[1 + 4^{-1} \ldots + 4^{3-\bar{\ell}}] = O(p^4 N/M)$$

(v) Evaluation of local expansions at leaf cells:

$$\text{CPU} = O(p^2 N/M)$$

(vi) Evaluation of near contributions $\mathcal{S}[\varphi, \partial\Omega]^{\text{near}}(\mathbf{x})$ using standard BEM techniques:

$$\text{CPU} = O((N/M) \times M \times |\mathcal{A}(\mathcal{C})|M) = O(|\mathcal{A}(\mathcal{C}_x)|MN)$$

Overall complexity: $\boxed{\text{CPU} = O(N)}$

Elastostatics

Reformulation of Kelvin solution in terms of $1/r$:

$$U_i^k(\mathbf{x},\boldsymbol{\xi}) = \frac{1}{16\pi\mu(1-\nu)}\Big\{(3-4\nu)\delta_{ik}\frac{1}{r} + (\xi_i - x_i)\frac{\partial}{\partial x_k}\frac{1}{r}\Big\} \qquad \text{(a)}$$

$$T_i^k(\mathbf{x},\boldsymbol{\xi}) = -\frac{1}{8\pi\mu(1-\nu)}\Big\{(1-2\nu)\big[n_k(\boldsymbol{\xi})\frac{\partial}{\partial x_i}\frac{1}{r} - n_i(\boldsymbol{\xi})\frac{\partial}{\partial x_k}\frac{1}{r}\big] + 2(1-\nu)\delta_{ik}n_j(\boldsymbol{\xi})\frac{\partial}{\partial x_j}\frac{1}{r} + (\xi_j - x_j)n_j(\boldsymbol{\xi})\frac{\partial^2}{\partial x_i \partial x_k}\frac{1}{r}\Big\} \qquad \text{(b)}$$

Substitute multipole expansion of $1/r$ into (a) and (b):

$$\frac{1}{\|\boldsymbol{\xi}-\mathbf{x}\|} = \sum_{n=0}^{+\infty}\sum_{m=-n}^{n} R_{n,m}(\mathbf{x}-\mathbf{x}_0)\sum_{n'=0}^{+\infty}\sum_{m'=-n'}^{n'}(-1)^n\overline{S_{n+n',m+m'}(\boldsymbol{\xi}_0-\mathbf{x}_0)}R_{n',m'}(\boldsymbol{\xi}-\boldsymbol{\xi}_0)$$

(again)

Elastostatics: multipole expansion of Kelvin solution

$$U_i^k(\mathbf{x},\boldsymbol{\xi}) = \frac{1}{16\pi\mu(1-\nu)} \sum_{n'=0}^{+\infty} \sum_{m'=-n'}^{n'} \Big\{ F_{ki}^{n',m'}(\mathbf{x}-\boldsymbol{\xi}_0) R_{n',m'}(\boldsymbol{\xi}-\boldsymbol{\xi}_0) + G_k^{n',m'}(\mathbf{x}-\boldsymbol{\xi}_0)(\xi_i-\xi_{i0}) R_{n',m'}(\boldsymbol{\xi}-\boldsymbol{\xi}_0) \Big\}$$

$$F_{ki}^{n',m'}(\mathbf{x}-\boldsymbol{\xi}_0) = \sum_{n=0}^{+\infty} \sum_{m=-n}^{n} (-1)^n \overline{S_{n+n',m+m'}(\boldsymbol{\xi}_0-\mathbf{x}_0)} \left[(3-4\nu)\delta_{ik} R_{n,m}(\mathbf{x}-\mathbf{x}_0) + (\xi_{i0}-x_{i0}-x_i-x_{i0}) \frac{\partial}{\partial x_k} R_{n,m}(\mathbf{x}-\mathbf{x}_0) \right]$$

$$G_k^{n',m'}(\mathbf{x}-\boldsymbol{\xi}_0) = \sum_{n=0}^{+\infty} \sum_{m=-n}^{n} (-1)^n \overline{S_{n+n',m+m'}(\boldsymbol{\xi}_0-\mathbf{x}_0)} \frac{\partial}{\partial x_k} R_{n,m}(\mathbf{x}-\mathbf{x}_0)$$

A similar formula (not shown) can be established for the multipole representation of $T_i^k(\mathbf{x},\boldsymbol{\xi})$

Elastostatics: multipole moments

$$M^{t}_{n',m';i}(\mathcal{C}_\xi;\boldsymbol{\xi}_0) = \int_{\partial\Omega\cup\mathcal{C}_\xi} R_{n',m'}(\boldsymbol{\xi}-\boldsymbol{\xi}_0)\ t_i(\boldsymbol{\xi})\,\text{d}S_\xi$$

$$M^{t}_{n',m'}(\mathcal{C}_\xi;\boldsymbol{\xi}_0) = \int_{\partial\Omega\cup\mathcal{C}_\xi} R_{n',m'}(\boldsymbol{\xi}-\boldsymbol{\xi}_0)\ (\xi_i-\xi_{i0})t_i(\boldsymbol{\xi})\,\text{d}S_\xi$$

$$M^{u}_{n',m';ki}(\mathcal{C}_\xi;\boldsymbol{\xi}_0) = \int_{\partial\Omega\cup\mathcal{C}_\xi} R_{n',m'}(\boldsymbol{\xi}-\boldsymbol{\xi}_0)\ n_k(\boldsymbol{\xi})u_i(\boldsymbol{\xi})\,\text{d}S_\xi$$

$$M^{u}_{n',m';k}(\mathcal{C}_\xi;\boldsymbol{\xi}_0) = \int_{\partial\Omega\cup\mathcal{C}_\xi} R_{n',m'}(\boldsymbol{\xi}-\boldsymbol{\xi}_0)\ n_k(\boldsymbol{\xi})(\xi_i-\xi_{i0})u_i(\boldsymbol{\xi})\,\text{d}S_\xi$$

M2M, M2L and L2L formulae

M2M, M2L and L2L formulae are derived using those for $1/r$. For example, the elastostatic M2M formulae are:

$$M^t_{n,m;i}(\mathcal{C}^{(\ell)}_\xi;\boldsymbol{\xi}^{(\ell-1)}_0) = \sum_{n'=0}^{\infty} \sum_{m'=-n'}^{n'} R_{n',m'}(\boldsymbol{\xi}^{(\ell)}_0 - \boldsymbol{\xi}^{(\ell-1)}_0) M^t_{n-n',m-m';i}(\mathcal{C}^{(\ell)}_\xi;\boldsymbol{\xi}^{(\ell)}_0)$$

$$M^t_{n,m}(\mathcal{C}^{(\ell)}_\xi;\boldsymbol{\xi}^{(\ell-1)}_0) = \sum_{n'=0}^{\infty} \sum_{m'=-n'}^{n'} \Big\{ R_{n',m'}(\boldsymbol{\xi}^{(\ell)}_0 - \boldsymbol{\xi}^{(\ell-1)}_0) M_{n-n',m-m'}(\mathcal{C}^{(\ell)}_\xi;\boldsymbol{\xi}^{(\ell)}_0) + (\xi^{(\ell)}_{i0} - \xi^{(\ell-1)}_{i0}) M^t_{n-n',m-m';i}(\mathcal{C}^{(\ell)}_\xi;\boldsymbol{\xi}^{(\ell)}_0)$$

$$M^u_{n,m;ki}(\mathcal{C}^{(\ell)}_\xi;\boldsymbol{\xi}^{(\ell-1)}_0) = \sum_{n'=0}^{\infty} \sum_{m'=-n'}^{n'} R_{n',m'}(\boldsymbol{\xi}^{(\ell)}_0 - \boldsymbol{\xi}^{(\ell-1)}_0) M_{n-n',m-m';ki}(\mathcal{C}^{(\ell)}_\xi;\boldsymbol{\xi}^{(\ell)}_0)$$

$$M^u_{n,m;k}(\mathcal{C}^{(\ell)}_\xi;\boldsymbol{\xi}^{(\ell-1)}_0) = \sum_{n'=0}^{\infty} \sum_{m'=-n'}^{n'} \Big\{ R_{n',m'}(\boldsymbol{\xi}^{(\ell)}_0 - \boldsymbol{\xi}^{(\ell-1)}_0) M_{n-n',m-m';k}(\mathcal{C}^{(\ell)}_\xi;\boldsymbol{\xi}^{(\ell)}_0) + (\xi^{(\ell)}_{i0} - \xi^{(\ell-1)}_{i0}) M^t_{n-n',m-m';ki}(\mathcal{C}^{(\ell)}_\xi;\boldsymbol{\xi}^{(\ell)}_0)$$

Numerical example: uniform thermal strain in ellipsoidal region

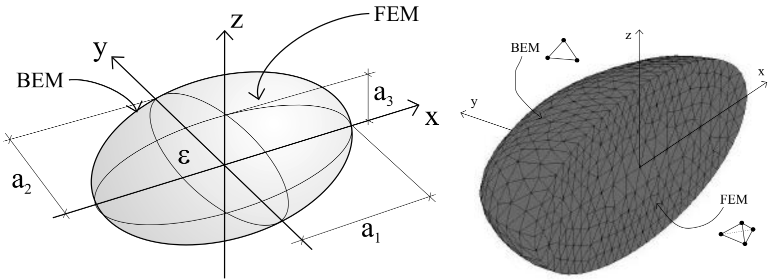

Mesh	Nodes	Elements		Oct-tree		DOFs		
		BEM	FEM	Max level	Leaves	N_{BEM}	N_{F}	$N_{\text{BEM}} + \text{N}_{\text{F}}$
1	267	346	979	3	42	1050	276	1326
2	822	1038	3153	3	100	3126	903	4029
3	1362	1540	5563	3	103	4632	1770	6402
4	2274	2418	9626	4	301	7266	3189	10455
5	5881	5200	26602	4	422	15612	9837	25449
6	12868	9402	61770	5	1175	28218	24495	52713
7	20258	12842	100200	6	1403	38538	41505	80043

Numerical example: uniform thermal strain in ellipsoidal region

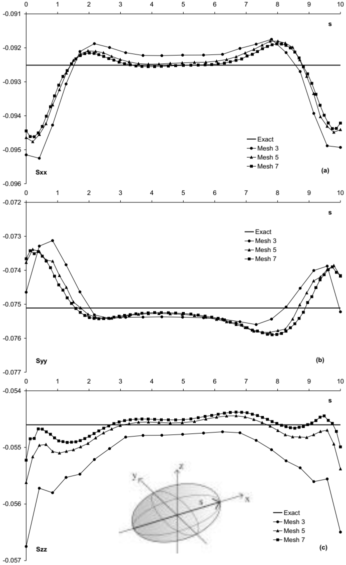

Mesh	Precond. (s) BEM	FEM	FMM (s/iter)	Iters n	Total time (s)
1	10	$<$1	1	37	43
2	36	$<$1	2	37	154
3	50	$<$1	3	37	202
4	64	3	6	36	277
5	169	18	11	37	721
6	349	101	19	38	1425
7	512	279	42	38	2913

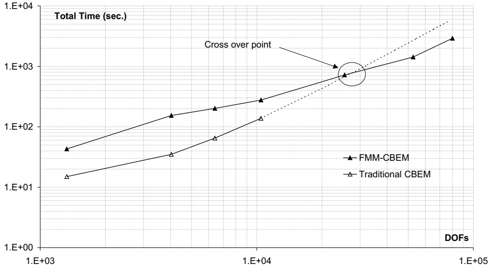

Numerical example: many-inclusion problem

Nodes	Elements		Oct-tree		DOFs		
	BEM	FEM	Max. level	Leaves	N_{BEM}	N_{F}	$N_{\text{BEM}} + \mathrm{N}_{\mathrm{F}}$
93227	122880	326493	5	7176	374784	92289	467073

Precond. (s)		Time (s)				Iters	Total time
BEM	FEM	Upw.	Downw.	Direct	Cycle	n	(s)
6609	19	47	48	84	180	147	39656

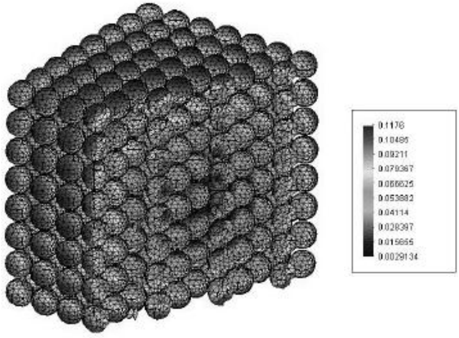

Numerical example: Pian Telessio dam

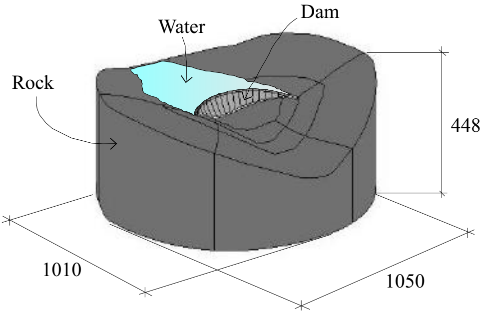

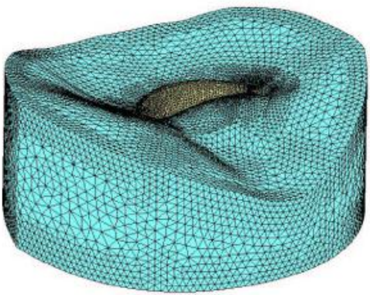

Numerical example: Pian Telessio dam

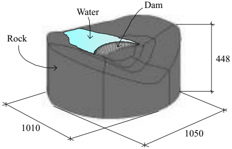

Mesh	Nodes	Elements		Oct-tree		DOFs		
		BEM	FEM	Levels	Leaves	N_{BEM}	N_{F}	Total
1	25443	21684 (T3)	73569 (T4)	9	8953	38118	43797	81915
2	23433	7726 (T6)	10307 (T10)	8	3548	50490	46773	97263
3	51978	15296 (T6)	14462 (T10)	8	6786	96636	64152	160788
A	406035	—	279742	—	—	—	—	1218105

Mesh	Precond. (s)		Time (s)				Iters	Total time
	BEs	FEs	Upw.	Down.	Direct	Cycle	n	(s)
1	186	26	23	27	24	76	83	7916
2	328	114	11	21	23	57	82	5818
3	1215	223	23	36	102	165	85	17775
A	—	—	—	—	—	—	—	3749

Numerical example: Pian Telessio dam

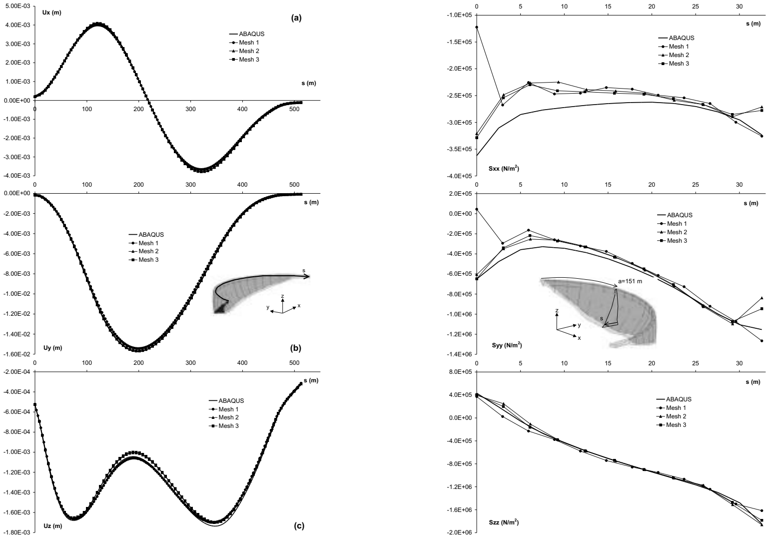

Exemple, calcul d'amortissements dans les MEMS

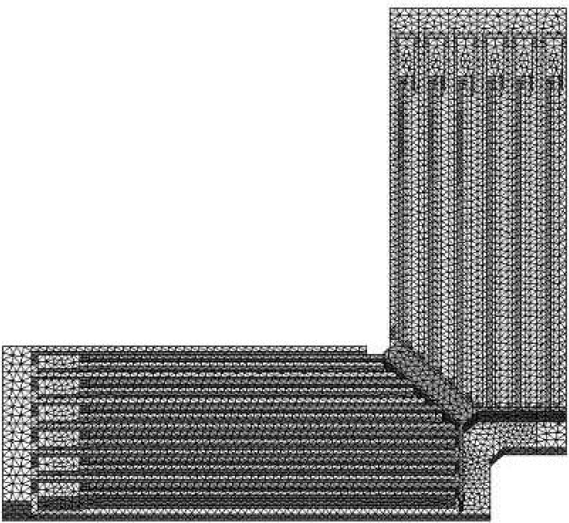

Figure 5. More realistic model of one-fourth of the MEMS: geometry and mesh.

Frangi A., Spinola G., Vigna B., IJNME **68**:1031–1051

Exemple, calcul d'amortissements dans les MEMS

Table II. Comparison between meshes of increasing refinement.

Mesh employed	Mesh 1	Mesh 2	Mesh 3
Number of unknowns	125 058	272 364	548 388
Global force (N)	1.80×10^{-4}	2.01×10^{-4}	2.12×10^{-4}

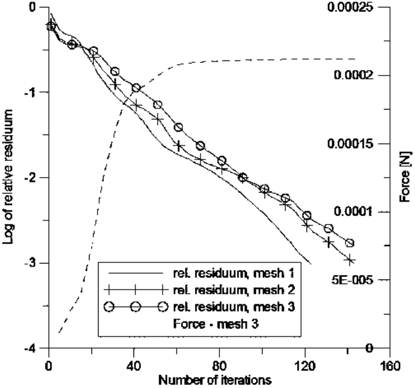

Figure 6. Convergence of the GMRES solver and of the force computed.

Frangi A., Spinola G., Vigna B., IJNME **68**:1031–1051

Exemple, homogénéisation numérique

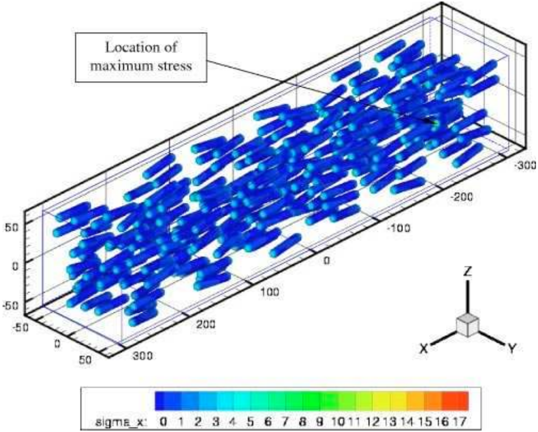

Fig. 10 **Contour plot of surface stresses** $(\times \sigma^{\infty})$ **for a model with 216 "randomly" distributed and oriented short fibers**

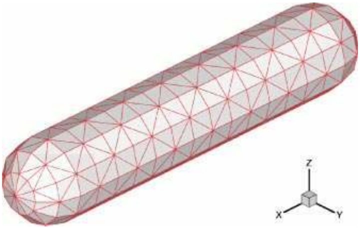

Fig. 9 **A BEM mesh used for the short fiber inclusion** (**with 456 elements**)

Liu Y.J., Nishimura N. et al., ASME J. Appl. Mech. **72**:115–128 (2005)

Exemple, homogénéisation numérique

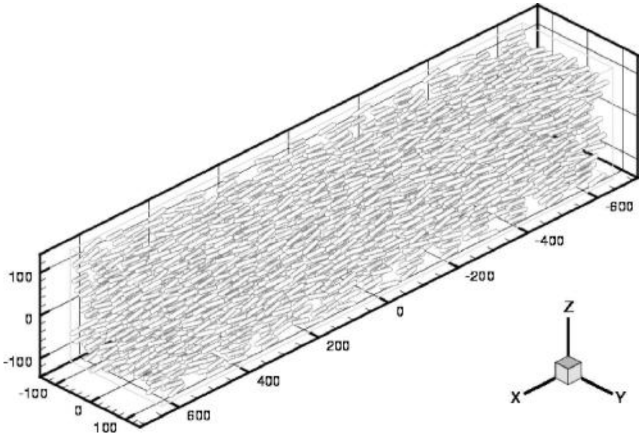

Fig. 11 A RVE containing 2197 short fibers with the total DOF=3 018 678

Liu Y.J., Nishimura N. et al., ASME J. Appl. Mech. **72**:115–128 (2005)

Exemple, homogénéisation numérique

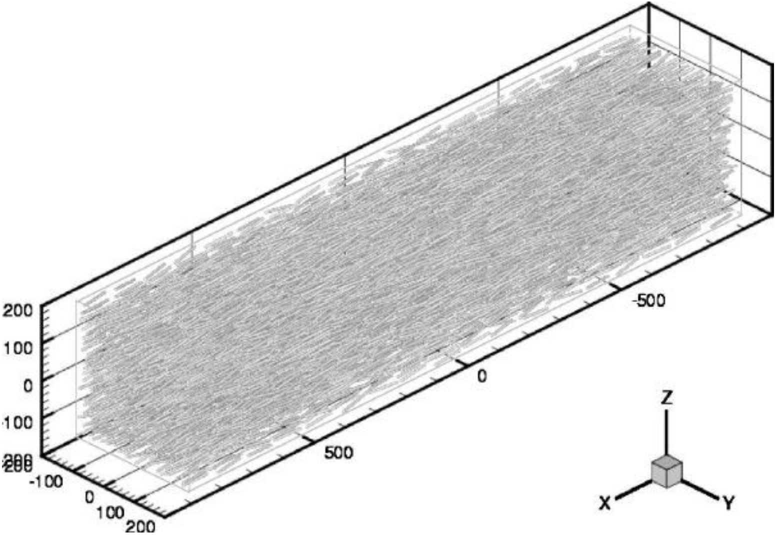

Fig. 14 A RVE containing 5832 long fibers with the total DOF=10 532 592

Liu Y.J., Nishimura N. et al., ASME J. Appl. Mech. **72**:115–128 (2005)

Exemple, homogénéisation numérique

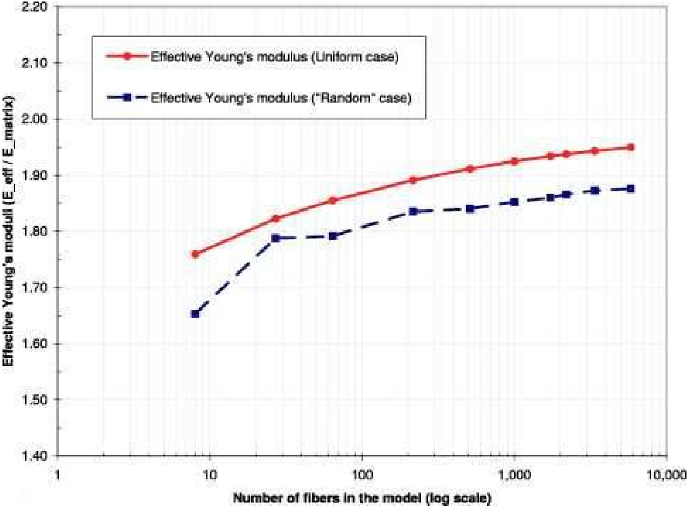

Fig. 15 **Estimated effective Young's moduli in the *x*-direction for the composite model with up to 5832 *long* rigid fibers (fiber volume fraction=3.85%)**

Liu Y.J., Nishimura N. et al., ASME J. Appl. Mech. **72**:115–128 (2005)

Avec: Jean-François Semblat (Civil Engineering Research Lab [LCPC], Paris)
Nicolas Nemitz (doctoral thesis, 2002-2006)
Stéphanie Chaillat (doctoral thesis, 2005–)
Eva Grasso (doctoral thesis, 2008–)
Tekoing Lim (doctoral thesis, Atomic Energy Commission [CEA], 2007–)

Motivation

Modelling of elastic wave propagation in large/unbounded domains

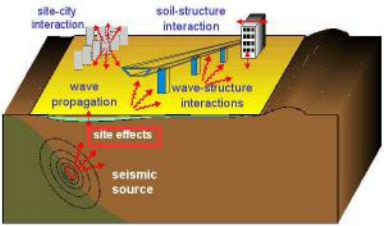

- Soil-structure interaction
- Site effects
- Computational forward solution method for inverse problems

Pros and cons of BEMs for elastic waves

FEM, FDM, DG...	BEM
→ Domain mesh	→ Surface mesh (i.e. reduced dimensionality)
→ Approx. radiation conditions	→ Exact radiation conditions
→ **Sparse** matrix	→ Fully-populated matrix

BEM adequate for large (unbounded) media with simple (linear) properties.
Fully-populated BEM influence matrix is a priori a severe limiting factor

Standard BEM (3-D elastodynamics, frequency domain)

Governing integral equation for boundary displacements and tractions

$$c_{ik}(\mathbf{x})u_i(\mathbf{x}) = \int_{\partial\Omega} \big[t_i(\mathbf{x}) U_i^k(\mathbf{x},\boldsymbol{\xi};\omega) - u_i(\mathbf{x}) T_i^k(\mathbf{x},\boldsymbol{\xi};\omega) \big] \, dS_\xi \qquad (\mathbf{x} \in \partial\Omega)$$

Full-space elastodynamic fundamental solutions

$$U_i^k(\mathbf{x},\boldsymbol{\xi};\omega) = \frac{1}{4\pi k_S^2 \mu} \Big((\delta_{qs}\delta_{ik} - \delta_{qk}\delta_{is}) \frac{\partial}{\partial x_q} \frac{\partial}{\partial y_s} G_S(\|\mathbf{x}-\boldsymbol{\xi}\|) + \frac{\partial}{\partial x_i} \frac{\partial}{\partial y_k} G_P(\|\mathbf{x}-\boldsymbol{\xi}\|) \Big)$$

$$T_i^k(\mathbf{x},\boldsymbol{\xi};\omega) = C_{ijh\ell} \frac{\partial}{\partial y_\ell} U_h^k(\mathbf{x},\boldsymbol{\xi};\omega) n_j(\boldsymbol{\xi})$$

$G_\alpha(z) = \dfrac{\exp(ik_\alpha z)}{z}$ (fund. sol. Helmholtz eqn., $\alpha = P, S$)

BEM discretization $\Longrightarrow$ fully-populated system of linear equations.

Computational limitations of standard BEM

Solution of fully-populated matrix equation

- Direct solvers (LU factorisation, ...) :
  - Pros: robust, accurate;
  - Cons: $O(N^2)$ memory and $O(N^3)$ CPU
- Iterative solvers (GMRES, ...) :
  - Pros: $O(N_{iter} \times N^2)$ CPU;
  - Cons: $O(N^2)$ memory; N_{iter} may be large

(N: number of BE DOFs)

Limitations of standard BEM

- High memory cost
  $\rightarrow$ problem size limit $N = O(10^4)$ (PC, single-proc.)
- Limited geometric complexity, (piecewise) heterogeneity, frequency range

Fast multipole accelerated BEM

Fast Multipole Method (FMM):

- Based on **iterative** linear equation solvers (GMRES)
- Fast method for evaluating matrix-vector products, i.e. discretized versions of e.g.

$$\int_{\partial\Omega} t_i(\mathbf{x}) U_i^k(\mathbf{x},\boldsymbol{\xi};\omega)\,\mathrm{d}S_\xi \qquad \text{(for given solution candidate } \mathbf{t}\text{)}$$

A few milestones

- Laplace: Rokhlin (1985)
- Electrostat.: Greengard (1988)
- Electromag.: Chew (1994), Darve (2000), Sylvand (2002)...
- Elastodyn. freq. domain: Fujiwara (2000)
- Elastodyn., time domain: Nishimura (2002)
- BEM-FEM : Margonari, Bonnet (2004), Gaul et al...
- Effective prop. of composite mater.: Nishimura, Liu (2005)

Decomposition of Helmholtz fundamental solution

Multipole expansion formula ("diagonal form", Epton and Dembart 1995)

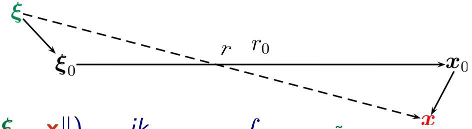

$$\frac{\exp(ik\|\boldsymbol{\xi}-\mathbf{x}\|)}{\|\boldsymbol{\xi}-\mathbf{x}\|} = \frac{ik}{4\pi}\lim_{L\to+\infty}\int_{\hat{\mathbf{s}}\in S} e^{ik\hat{\mathbf{s}}.\tilde{\boldsymbol{\xi}}}\mathcal{G}_L(\hat{\mathbf{s}};\mathbf{r}_0;k)e^{-ik\hat{\mathbf{s}}.\tilde{\mathbf{x}}}d\hat{\mathbf{s}}$$

Transfer function

$$\mathcal{G}_L(\hat{\mathbf{s}};\mathbf{r}_0;k) = \sum_{p=0}^{L}(2p+1)i^p h_p^{(1)}(k\|\mathbf{r}_0\|)P_p\big(\cos(\hat{\mathbf{s}},\mathbf{r}_0)\big)$$

Single-level FMM

Boundary of interest enclosed in cubic grid

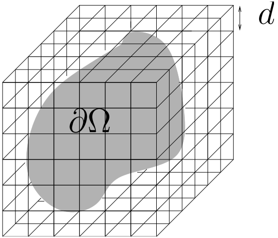

Convergence of multipole expansion assured if **x** and $\boldsymbol{\xi}$ lie in non-adjacent cells

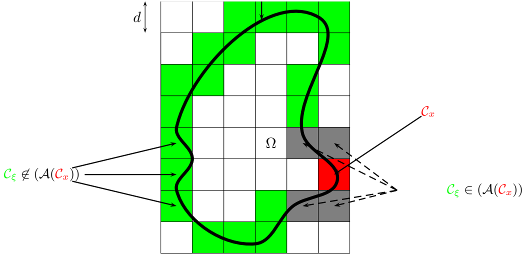

Single-level FMM

Matrix-vector product $\longleftarrow$ evaluation of integral operator

- Must compute e.g.:

$$[\mathcal{K}\{t\}](\mathbf{x}) := \int_{\partial\Omega} t_i(\mathbf{x}) U_i^k(\mathbf{x}, \boldsymbol{\xi}; \omega) \, \mathrm{d}S_\xi \qquad \text{(for given solution candidate } \mathbf{t}\text{)}$$

- Split integrals into near and FM contributions:

$$\int_{\partial\Omega} = \sum_{\mathcal{C}_\xi \in \mathcal{A}(\mathcal{C}_x)} \int_{\partial\Omega \cap \mathcal{C}_\xi} + \sum_{\mathcal{C}_\xi \notin \mathcal{A}(\mathcal{C}_x)} \int_{\partial\Omega \cap \mathcal{C}_\xi}$$

$$[\mathcal{K}\{t\}](\mathbf{x}) = [\mathcal{K}\{t\}]^{\text{near}}(\mathbf{x}) + [\mathcal{K}\{t\}]^{\text{far}}(\mathbf{x})$$

Single-level FMM algorithm: principle

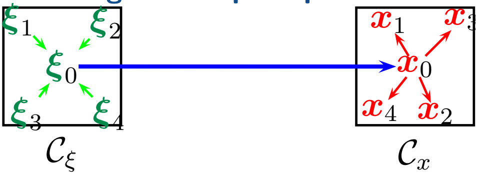

$$\int_{\partial\Omega} t_i(\mathbf{x}) U_i^k(\mathbf{x},\xi;\omega)\,\mathrm{d}S_\xi \qquad \text{(for given solution candidate } \mathbf{t}\text{)}$$

$$\frac{\exp(ik\|\xi-\mathbf{x}\|)}{\|\xi-\mathbf{x}\|} = \frac{ik}{4\pi}\lim_{L\to+\infty}\int_{\hat{\mathbf{s}}\in S} e^{ik\hat{\mathbf{s}}.\tilde{\xi}}\mathcal{G}_L(\hat{\mathbf{s}};\mathbf{r}_0;k)e^{-ik\hat{\mathbf{s}}.\tilde{\mathbf{x}}}d\hat{\mathbf{s}}$$

- compute multipole moments for each cell $\mathcal{C}_\xi$ and quadrature point
- Transfer (M2L) from $\mathcal{C}_\xi$ to non-adjacent $\mathcal{C}_x$
- Evaluate FM contribution to matrix-vector product
- Add near contribution to matrix-vector product (computed using standard BEM techniques)

Complexity of single-level elastodynamic FMM: $O(N^{3/2})$ per GMRES iteration

Multi-level FMM

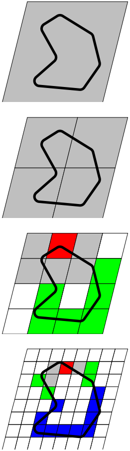

level $\ell = 0$

level $\ell = 1$

level $\ell = 2$ $\rightarrow$ highest level for which FMM is applicable.

level $\ell = 3$

$\vdots$

level $\ell = \bar{\ell}$ (leaf)

computation organization based on recursive subdivision (oc-tree)

Complexity of multi-level elastodynamic FMM: $O(N \log_2 N)$

Computational issues: truncation of transfer function

Transfer function

$$\mathcal{G}_L(\hat{\mathbf{s}};\mathbf{r}_0;k)=\sum_{p=0}^{L}(2p+1)i^p h_p^{(1)}(k\|\mathbf{r}_0\|)P_p\big(cos(\hat{\mathbf{s}},\mathbf{r}_0)\big)$$

Choice of truncation parameter:

- L too small: convergence not reached for $\mathcal{G}_L(\hat{\mathbf{s}};\mathbf{r}_0;k)$;
- L too large: divergence of $h_p^{(1)}$

Empirical formula used

L$=\sqrt{3}k_S d+C_\epsilon log_{10}(\sqrt{3}k_S d+\pi)$
(see Darve 2000 and Sylvand 2002 for Maxwell eqns)

Computational issues: adjustment of constant C_ϵ

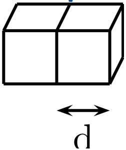

$$L = \sqrt{3}k_S d + C_\epsilon log_{10}(\sqrt{3}k_S d + \pi)$$

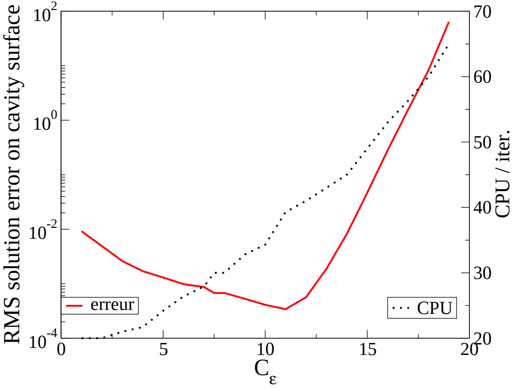

$\longrightarrow C_\epsilon = 7.5$ (consistent with Sylvand 2002, Maxwell eqns)

Computational issues: number of levels

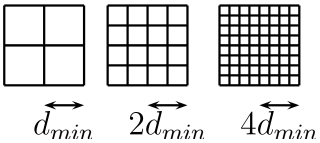

$$L = \sqrt{3}k_S d + C_\epsilon log_{10}(\sqrt{3}k_S d + \pi)$$

# of levels	$d_{min} \times k_S/2\pi$	rel. err. / BEM	CPU / iter (s)
4	1.32	$1.1\ .10^{-5}$	367
5	0.66	$4.7\ .10^{-4}$	134
6	0.33	$3.7\ .10^{-3}$	104
7	0.17	$5.1\ .10^{-2}$	200
8	0.083	$1.7\ .10^{-1}$	380

Choice of leaf cell size ($\Leftrightarrow$ choice of # of levels):

- influence on CPU
- influence on accuracy

$\rightarrow d_{min} \geq 0.3 \times \lambda_S$

Computational issues: discretization relative to wavelength

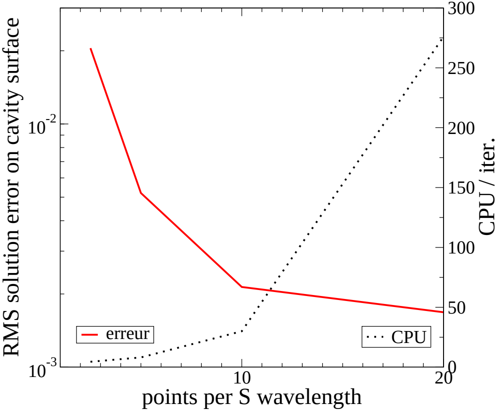

$\rightarrow$ 10 points per S wavelength

Numerical verification of theoretical complexity (CPU), Helmholtz

Example: sphere under uniform normal velocity. Mesh refinement, mesh density / wavelength kept fixed

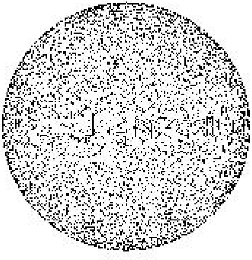

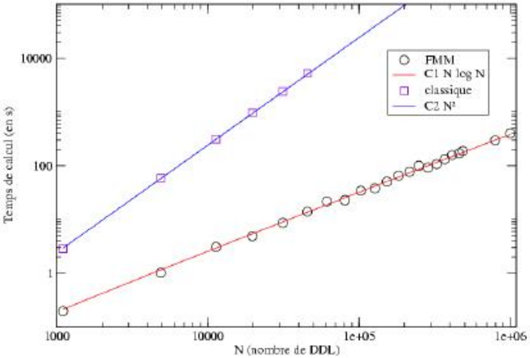

N. Nemitz, M. Bonnet, *Eng. Anal. Bound. Elem* (2008)

Numerical verification of theoretical complexity (CPU), elastodynamics

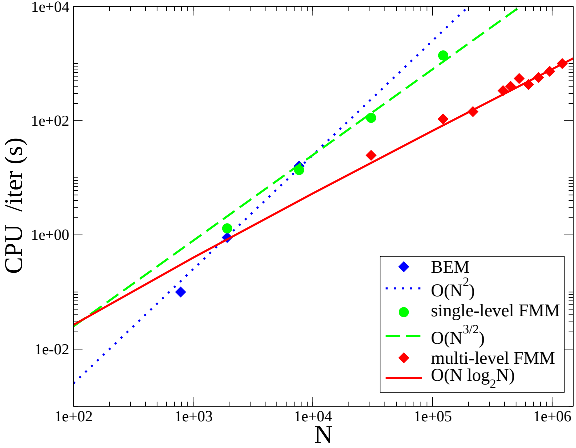

Chaillat S., Bonnet M., Semblat J.F., *Comp. Meth. Appl. Mech. Engng.* (2008)

Example (Helmholtz)

Identification of a dual hard scatterer

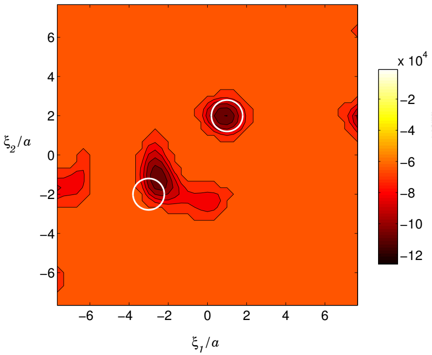

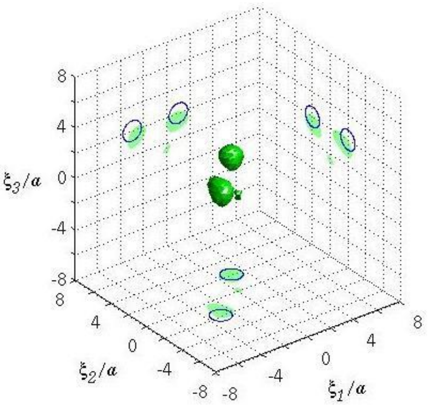

N. Nemitz, M. Bonnet, *Eng. Anal. Bound. Elem* (2008).

Example (Helmholtz)

FMM: numerical parameters

Element and DOF count (FM-BEM):

Cube size	Cube		Obstacle		Total		$\mathcal{G}$
	Elements	DDLs	Elements	DDLs	Elements	DDLs	
$16a$	76800	38402	336	170	77136	38572	100^3
$32a$	307200	153602	336	170	307536	153772	150^3

CPU timing (single-CPU PC) and GMRES iteration count

Cube size	u_{true} on $S \cup \Gamma_{\text{true}}$	u on S	$\hat{u}$ on S	$\mathcal{T}$ on $\mathcal{G}$
$16a$	$1444s$ ($N_{\text{iter}} = 435$)	969s ($N_{\text{iter}} = 282$)	1163s ($N_{\text{iter}} = 342$)	852s
$32a$	$6461s$ ($N_{\text{iter}} = 439$)	5615s ($N_{\text{iter}} = 388$)	6818s ($N_{\text{iter}} = 476$)	1860s

N. Nemitz, M. Bonnet, *Eng. Anal. Bound. Elem* (2008).

Example: scattering of a plane P wave by a spherical cavity

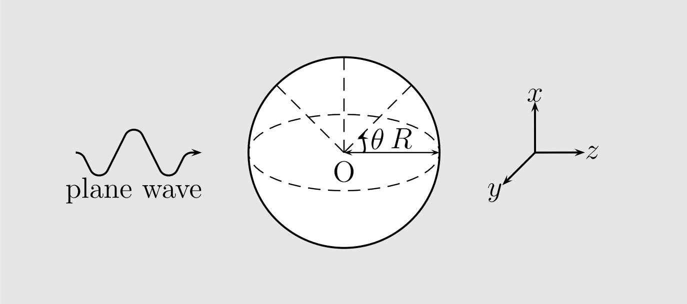

Chaillat S., Bonnet M., Semblat J.F., *Comp. Meth. Appl. Mech. Engng.* (2008)

Example: scattering of a plane P wave by a spherical cavity

$\theta = 0$

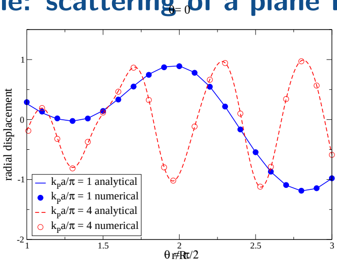

$\theta = \pi/4$

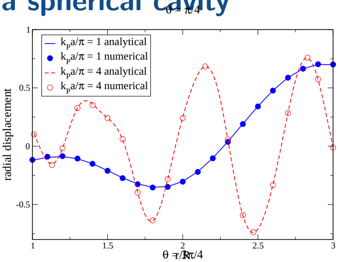

$\theta = \pi/2$

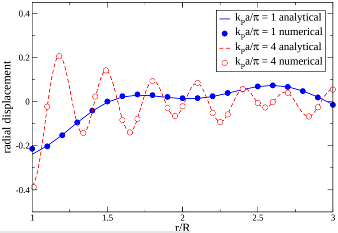

$\theta = 3\pi/4$

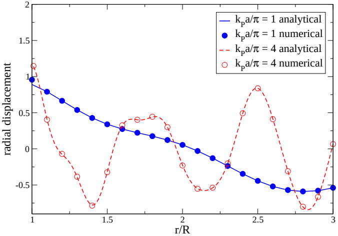

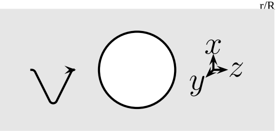

$N = 122,886$

Example: scattering of a plane P wave by a hemispheric canyon

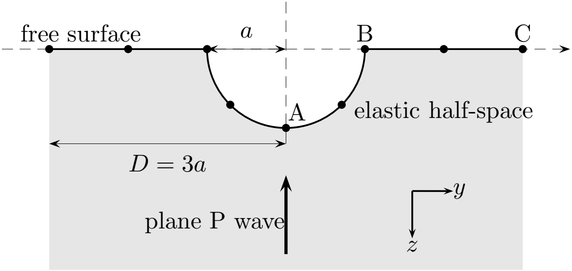

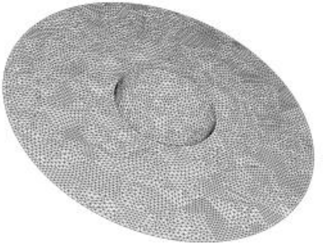

($N = 23382$)

- Simplified configuration for topographic site effect
- Low frequency: comparison with other published results
- Higher frequency: FMM

Chaillat S., Bonnet M., Semblat J.F., *Comp. Meth. Appl. Mech. Engng.* (2008)

Example: scattering of a plane P wave by a hemispheric canyon

Comparaison with earlier results, $k_P a = 0.25$ (low frequency)

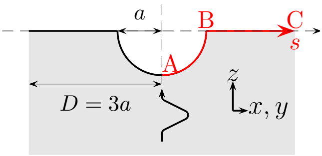

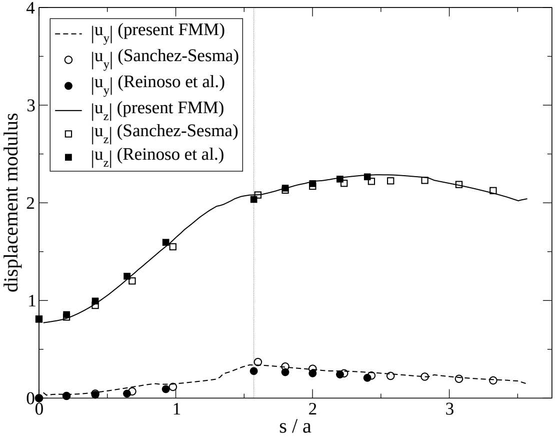

Example: scattering of a plane P wave by a hemispheric canyon

Results for higher frequency $k_P a = 5$
$N = 287\ 946$ (86 iter., 210 s / iter, single-proc. 3 GHz PC)

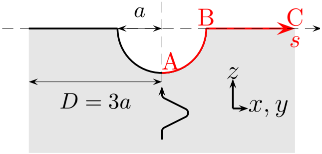

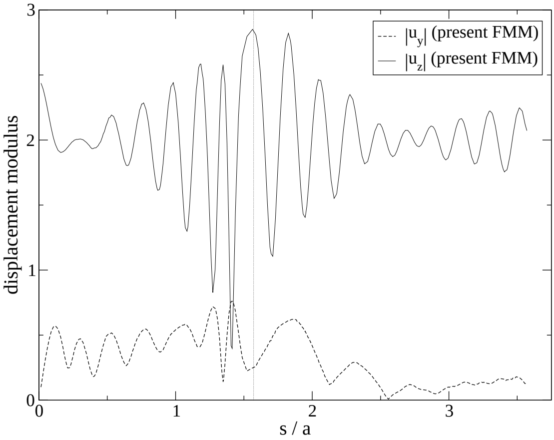

Example: scattering of a plane P wave by a hemispheric canyon

Study of convergence of GMRES

	$k_P a = 0.25$	$k_P a = 0.5$	$k_P a = 0.75$	$k_P a = 1.5$	$k_P a = 5$	$k_P a = 10$
$D = 3a$	**7** (23382)	**10** (23382)	**12** (23382)	**19** (23382)	**86** (287946)	> 280 (114570
$D = 5a$	**7** (61875)	**10** (61875)	**15** (61875)	**28** (61875)	**159** (774180)	
$D = 7a$	**8** (77565)	**13** (77565)	**17** (77565)	**43** (77565)		
$D = 20a$	**14** (98844)	**39** (98844)	**43** (98844)			

Example: scattering of a plane P wave by a semi-elliptical canyon

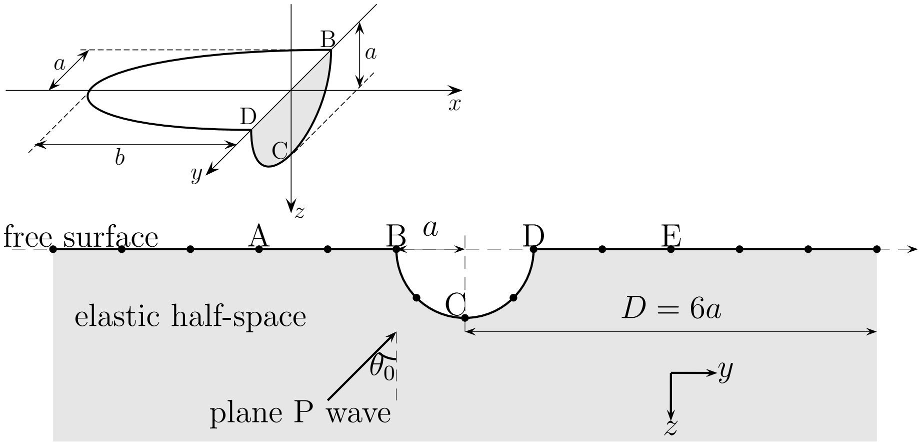

- Simplified configuration for topographic site effect
- Low frequency: comparison with other published results
- Higher frequency: FMM

Example: scattering of a plane P wave by a semi-elliptical canyon

Comparaison with earlier results, $k_S a = 0.5$ (low frequency), $N = 25\,788$

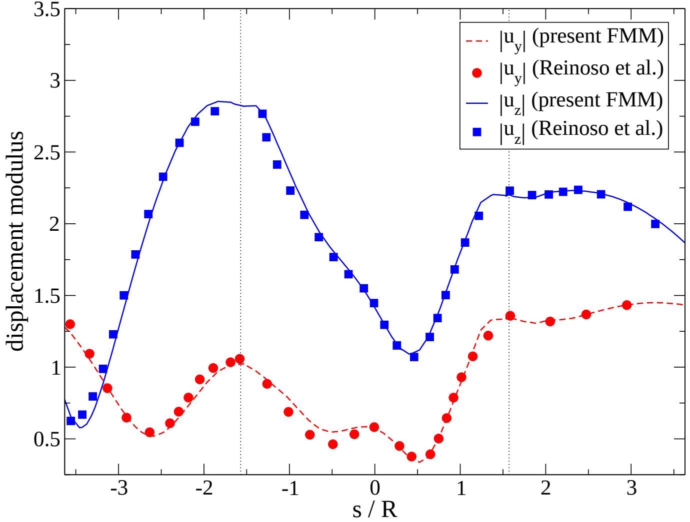

Example: scattering of a plane P wave by a semi-elliptical canyon

Results for higher frequency $k_s a = 2$

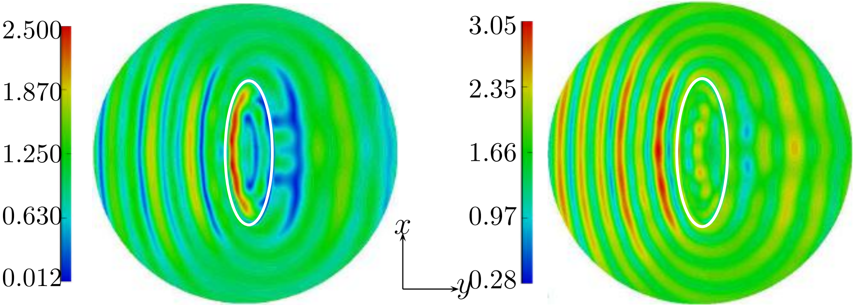

$N = 353\,232$ (32 iter., 140 s / iter, single-proc. 3 GHz PC)

Example: scattering of a plane P wave by an alluvial hemispheric valley

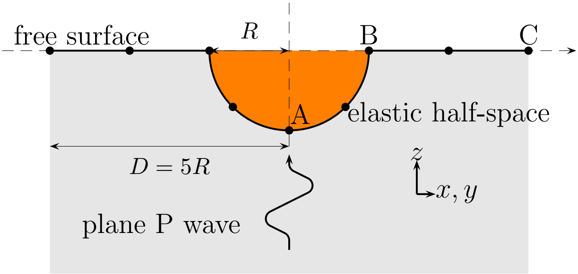

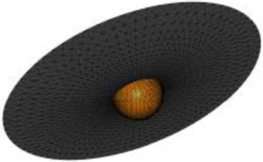

$(N = 17409)$

- $\mu_2 = 0.3\mu_1$, $\rho_2 = 0.6\rho_1$, $\nu_1 = 0.25$, $\nu_2 = 0.3$
- Low frequency: comparison with Sanchez-Sesma (1983) and Delavaud (2007)
- Higher frequency: FMM

Example: scattering of a plane P wave by an alluvial hemispheric valley

Comparaison with earlier results, $k_P R = 0.5$

- Sanchez-Sesma, 1983 (semi-analytical)
- Delavaud, 2007 (spectral finite element method)

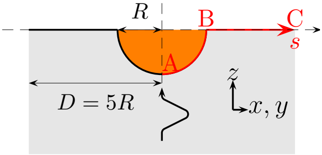

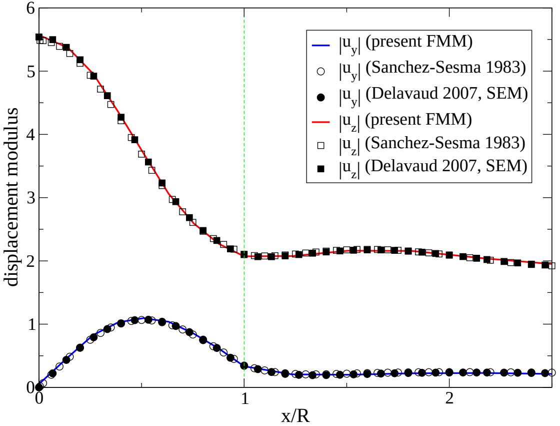

Example: scattering of a plane P wave by an alluvial hemispheric valley

Comparaison with earlier results, $k_P R = 0.7$:

- Sanchez-Sesma, 1983 (semi-analytical)
- Delavaud, 2007 (spectral finite element method)

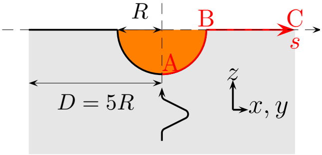

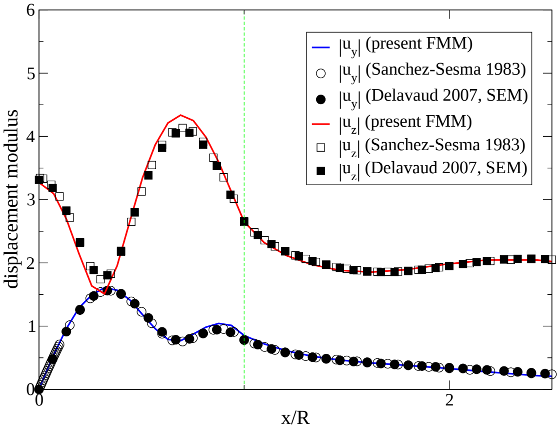

Example: scattering of a plane P wave by an alluvial hemispheric valley

Results for a higher frequency $k_P R = 1$
$N = 84\ 882$ (76 iterations, single-proc. 3 GHz PC)

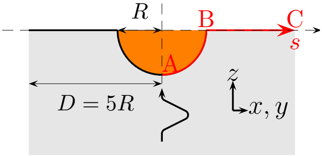

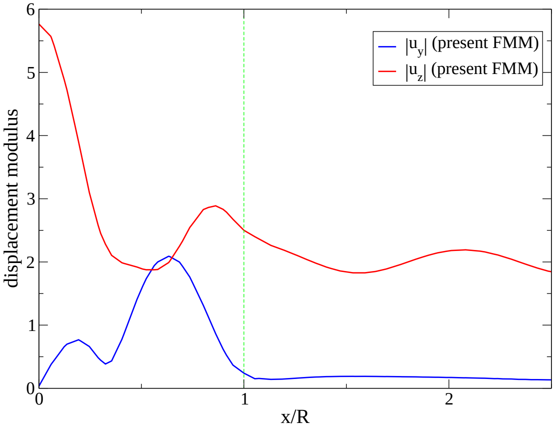

Exponential representation of $1/r$

- Partial Fourier transform along (ξ_1, ξ_2) coordinates (η_1, η_2 transformed variable):

$$\Delta G(\mathbf{x}, \cdot) + \delta(\cdots - \mathbf{x}) = 0 \quad \Longrightarrow \quad \hat{G}_{,33} - \eta^2 \hat{G} + \frac{e^{-\mathrm{i}\boldsymbol{\eta}.\mathbf{x}}}{4\pi^2}\delta(\xi_3 - x_3) = 0$$

- Solve analytically for $\hat{G}(\eta_1, \eta_2, \xi_3; \mathbf{x})$ (case $(\xi_3 > x_3)$):

$$\hat{G}(\eta_1, \eta_2, \xi_3; \mathbf{x}) = \frac{1}{8\pi^2} \exp\big[-\eta(\xi_3 - x_3) + \mathrm{i}\big(\eta_1(\xi_1 - x_1) + \eta_2(\xi_2 - x_2)\big) \big]$$

- Exponential representation of $1/r$ (case $\xi_3 > x_3$):

$$\frac{1}{\|\boldsymbol{\xi} - \mathbf{x}\|} = \frac{1}{2\pi} \int_0^{+\infty} \int_0^{2\pi} e^{-\eta[\,(\xi_3 - x_3) - \mathrm{i}(\,\cos\alpha(\xi_1 - x_1) + \sin\alpha(\xi_2 - x_2)\,)\,]} \, \mathrm{d}\alpha \mathrm{d}\eta$$

- Similar (but distinct) formula available for the case $\xi_3 < x_3$.

- Cheng, H., Greengard, L., Rokhlin, V. A fast adaptive multipole algorithm in three dimensions. *J. Comp. Phys.*, **155**:468–498 (1999).

Exponential representation of $1/r$

$$\frac{1}{\|\boldsymbol{\xi}-\mathbf{x}\|} = \frac{1}{2\pi}\int_0^{+\infty}\int_0^{2\pi} e^{-\eta[\,(\xi_3-x_3)-\mathrm{i}(\,\cos\alpha(\xi_1-x_1)+\sin\alpha(\xi_2-x_2)\,)\,]}\,\mathrm{d}\alpha\mathrm{d}\eta \qquad (\xi_3 > x_3)$$

Division of interaction list into 6 (3-D) or 4 (2-D) sublists:

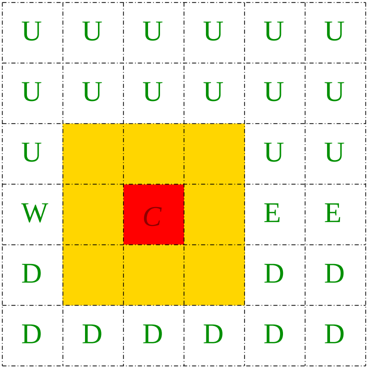

- Uplist (U)
- Downlist (D)
- Eastlist (E)
- Westlist (W)
- Northlist (N), for 3-D
- Southlist (S), for 3-D

Exponential representation of $1/r$: numerical quadrature

$$\left| \frac{1}{\|\boldsymbol{\xi}-\mathbf{x}\|} - \sum_{k=1}^{s_\epsilon} \frac{w_k}{M_k} \sum_{j=1}^{M_k} e^{-\eta_k[\,(\xi_3-x_3)-\mathrm{i}(\,\cos\alpha_{j,k}(\xi_1-x_1)+\sin\alpha_{j,k}(\xi_2-x_2)\,)\,]} \right| < \epsilon$$

- Outer numerical quadrature: points η_k and weights w_k given by Cheng, Rokhlin, Yarvin (1999);
- Inner numerical quadrature: M_k equally-spaced angles $\alpha_{j,k} = 2\pi j/M_k$, with M_k also given by Cheng, Rokhlin, Yarvin (1999).
- Comparison with "traditional" multipole expansion:

$$\boxed{M_1 + \ldots + M_{s_\epsilon} = O(p_\epsilon^2)}$$

- Cheng, H., Rokhlin, V., Yarvin, N. Nonlinear optimization, quadrature and interpolation. *SIAM J. Optim.*, **9**:901–923 (1999).

Exponential representation of $1/r$ and diagonal translations

$$\left| \frac{1}{\|\boldsymbol{\xi}-\mathbf{x}\|} - \sum_{k=1}^{s_\epsilon} \frac{w_k}{M_k} \sum_{j=1}^{M_k} e^{-\eta_k[\ (\xi_3 - x_3) - \mathrm{i}(\ \cos\alpha_{j,k}(\xi_1 - x_1) + \sin\alpha_{j,k}(\xi_2 - x_2)\ )\ ]} \right| < \epsilon$$

Insert poles $\mathbf{x}, \xi$, define multipole moments and translation operations.

- Multipole moments:

$$M(k,j) = \int_{\partial\Omega \cup \mathcal{C}_\xi} e^{-\eta_k[\ (\xi_3 - \xi_{3,0}) - \mathrm{i}(\ \cos\alpha_{j,k}(\xi_1 - \xi_{10,}) + \sin\alpha_{j,k}(\xi_2 - \xi_{2,0})\ )\ ]} \phi(\boldsymbol{\xi})\, \mathrm{d}S_\xi$$

- M2M, M2L, L2L translations are diagonal, e.g.:

$$L(k,j) = M(k,j)\, e^{-\eta_k[\ (\xi_{3,0} - x_{3,0}) - \mathrm{i}(\ \cos\alpha_{j,k}(\xi_{1,0} - x_{1,0}) + \sin\alpha_{j,k}(\xi_{2,0} - x_{2,0})\ )\ ]}$$

  Speeds up M2M, M2L, L2L operations
  ($O(p^2N)$ instead of $O(p^4N)$ using "traditional" FMM)
- Summation w.r.t. (k, i) performed on local expansions, at the very end (after upward, M2L and downward phases)
- Exponential expansions available for other kernels, e.g. Helmholtz
  Useful for FMM for low-frequency wave problems

FMM using equivalent sources

Main idea: express fields at remote points in terms of equivalent density, e.g.:

$$\int_{\partial\Omega\cap\mathcal{C}_\xi} G_{,n}(\mathbf{x},\boldsymbol{\xi})u(\boldsymbol{\xi})\,\mathrm{d}S_\xi = \int_{S_d} G(\mathbf{x},\mathbf{z})\phi(\mathbf{z})\,\mathrm{d}S_z \quad \text{for some } \phi \qquad (\mathbf{x}\notin\mathcal{A}(\mathcal{C}_\xi))$$

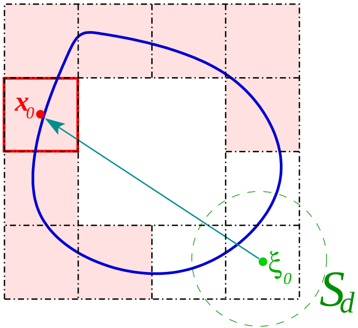

- YING, L., BIROS, G., ZORIN, D. A kernel-independent adaptive fast multipole in two and three dimensions. *J. Comp. Phys.*, **196**:591–626 (2004).

FMM using equivalent sources

Main idea: express fields at remote points in terms of equivalent density, e.g.:

$$\int_{\partial\Omega\cap\mathcal{C}_\xi} G_{,n}(\mathbf{x},\boldsymbol{\xi})u(\boldsymbol{\xi})\,\mathrm{d}S_\xi = \int_{S_d} G(\mathbf{x},\mathbf{z})\phi(\mathbf{z})\,\mathrm{d}S_z \quad \text{for some } \phi \qquad (\mathbf{x}\in S_c)$$

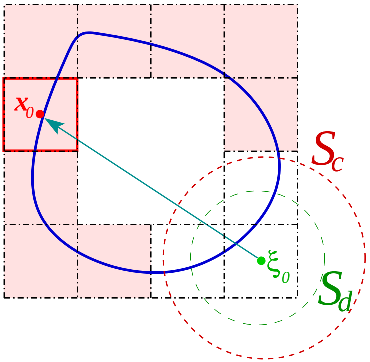

- Solve the above (Fredholm, 1st kind) integral equation for ϕ
- Truncation parameter = discretization of ϕ

FMM using equivalent sources: M2M translations

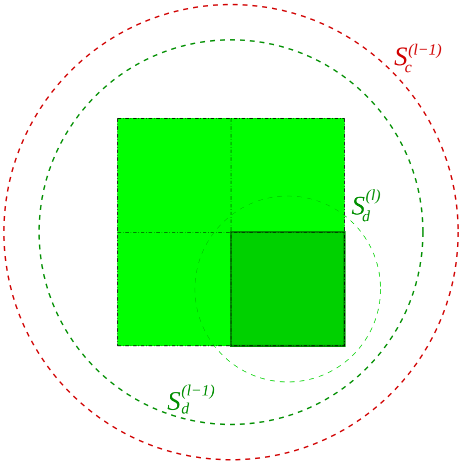

Find $\phi^{(\ell-1)}$, $\quad \displaystyle\int_{S_d^{(\ell-1)}} G(\mathbf{x},\mathbf{z})\phi^{(\ell-1)}(\mathbf{z})\,\mathrm{d}S_z = \int_{S_d^{(\ell)}} G(\mathbf{x},\mathbf{z})\phi^{(\ell)}(\mathbf{z})\,\mathrm{d}S_z \quad (\mathbf{x}\in S_c^{(\ell-1)})$

FMM using equivalent sources: L2L translations

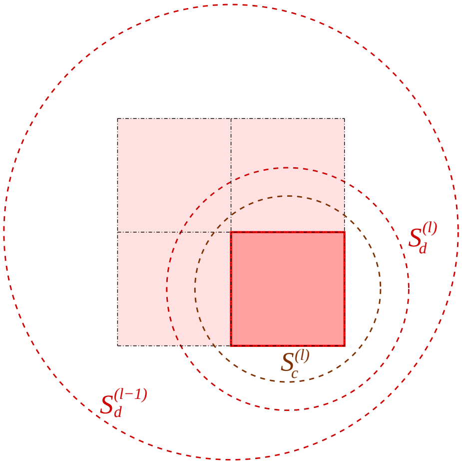

Find $\phi^{(\ell)}$, $\quad \displaystyle\int_{S_d^{(\ell)}} G(\mathbf{x},\mathbf{z})\phi^{(\ell)}(\mathbf{z})\,\mathrm{d}S_z = \int_{S_d^{(\ell-1)}} G(\mathbf{x},\mathbf{z})\phi^{(\ell-1)}(\mathbf{z})\,\mathrm{d}S_z \quad (\mathbf{x}\in S_c^{(\ell)})$

FMM using equivalent sources

- Kernel-independent acceleration method;
- Truncation parameter $p =$ discretization of ϕ (scale-independent for kernels associated with elliptic problems);
- Found by Ying, Biros, Zorin (2004) to have $O(p^2N)$ complexity / iteration;
- Requires solving 1st kind integral equations (ill-conditioned integral operator)

DOF clustering

- Spatially local DOFs (e.g. nodal values on a BEM mesh);
- Recursive subdivision of set of DOFs into subsets, e.g. by bisection

Example (1-D BE mesh, e.g for a 2-D crack problem):

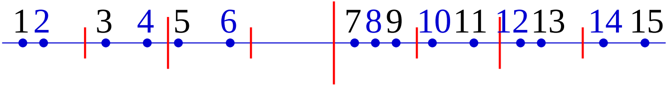

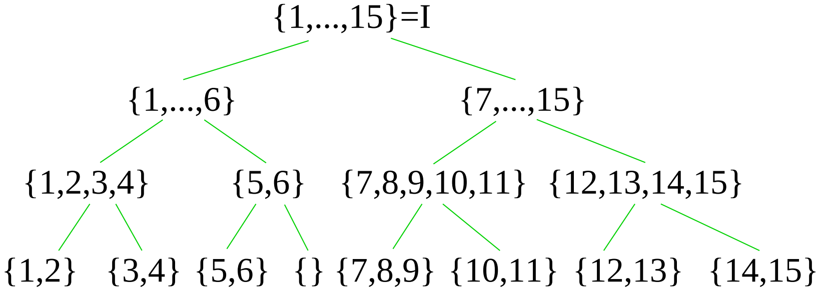

Block clustering of influence matrix

- Let Ω_1, Ω_2 denote the geometrical support of two clusters (i.e. of two subsets of the DOF index list $\mathcal{K}$). For instances, Ω_1, Ω_2 are cubic cells.
  Ω_1, Ω_2 are **admissible** if

$$\text{Min}\big(\text{Diam}(\Omega_1), \text{Diam}(\Omega_2)\big) \leq \eta \text{Dist}(\Omega_1, \Omega_2)$$

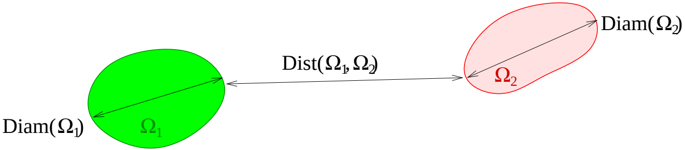

- Block clustering of (BEM) influence matrix into n blocks:

$$(I_1 \times J_1) \cup \ldots \cup (I_n \times J_n) = \mathcal{K} \times \mathcal{K}, \qquad I_k, J_k \text{generated by DOF clustering of } \mathcal{K}$$

  Such block clustering is not unique for a given index set $\mathcal{K}$.
- **Hierarchical, recursive** block clustering of (BEM) influence matrix into n blocks:
  $\longrightarrow$Block $\mathcal{K} \times \mathcal{K}$ is not admissible.
  $\longrightarrow$If block $(I \times J)$ is admissible, do nothing
  Else, create sub-blocks of $(I \times J)$ using children sublists of (I, J)

Block clustering of influence matrix: example

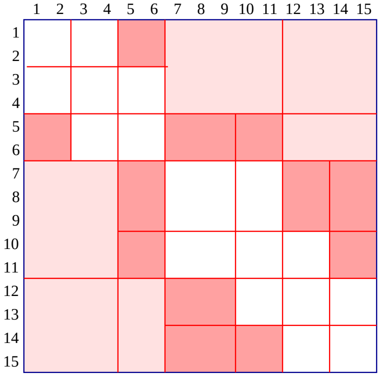

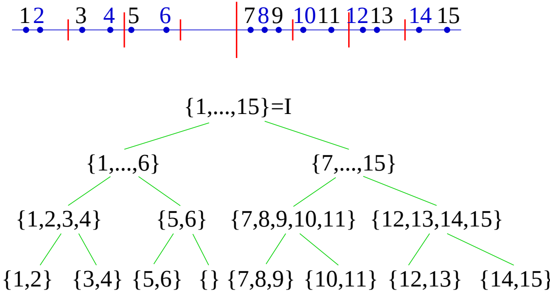

Concept of panel clustering in the BEM (Hackbusch and Nowak, 1989)
Concept of $\mathcal{H}$-matrices (Hackbusch, 1999)

Acceleration via low-rank approximation of blocks

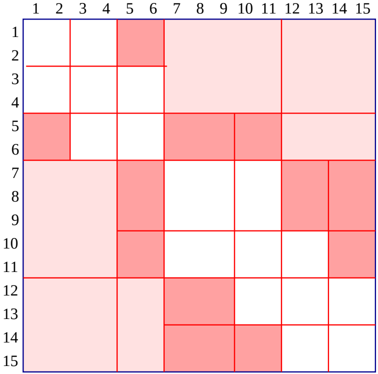

Idea: use **low-rank approximations** of blocks:

$$\mathbf{A}(I,J) \approx \sum_{k=1}^{r} \mathbf{a}_k \mathbf{b}_k^{\mathsf{T}}$$

Ideally, $r \ll |I|, |J|$
Matrix-vector product:

$$\mathbf{A}(I,J)\mathbf{u}(I) \approx \sum_{k=1}^{r} \big(\mathbf{b}_k^{\mathsf{T}}\mathbf{u}(I)\big)\mathbf{u}(I)$$

Block clustering + low-rank approximation of blocks = acceleration of matrix operations

SVD and block rank

- **Any** block $\mathbf{A}(I,J)$ of size $m \times n$ admits a **singular value decomposition** (SVD):

$$\mathbf{A}(I,J) = \mathbf{U}\mathbf{S}\mathbf{V}^{\mathsf{T}} = \sum_{k=1}^{R} s_k\, \mathbf{u}_k \mathbf{v}_k^{\mathsf{T}} \qquad s_1 \geq s_2 \geq \ldots s_R > 0,\ \mathbf{u}_k^{\mathsf{T}}\mathbf{u}_\ell = \mathbf{v}_k^{\mathsf{T}}\mathbf{v}_\ell = \delta_{k\ell}$$

  $R \leq \text{Min}(m,n)$ is the (numerical) **rank** of $\mathbf{A}(I,J)$
- $\mathbf{A}(I,J)$ has (approximate) low rank r if s_k is sufficiently small for $k > r$
- Computing complete SVD of $\mathbf{A}(I,J)$ needs $O(mn)$ memory + $O(mn^2)$ CPU
  not acceptable; other strategies required
  $\longrightarrow$FMM (analytic decomposition of kernel required)
  $\longrightarrow$Kernel interpolation (analytic decomposition of kernel not required)
  $\longrightarrow$Algebraic treatment of matrix blocks: adaptive cross approximation
  $\longrightarrow$Wavelet transformation of basis functions (not addressed here)

FMM as block clustering with low-rank approximation of blocks

The multi-level Fast Multipole Method features **block clustering** (through hierarchical octree of cubic cells)

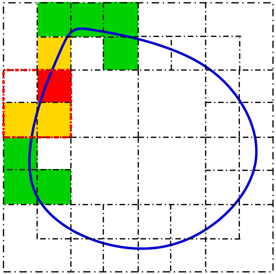

and **low-rank approximation** through **truncated** multipole expansion

$$\frac{1}{\|\boldsymbol{\xi}-\mathbf{x}\|} = \sum_{n=0}^{p} \sum_{m=-n}^{n} R_{n,m}(\mathbf{x}-\mathbf{x}_0) \sum_{n'=0}^{p} \sum_{m'=-n'}^{n'} (-1)^n \overline{S_{n+n',m+m'}(\boldsymbol{\xi}_0-\mathbf{x}_0)} R_{n',m'}(\boldsymbol{\xi}-\boldsymbol{\xi}_0)$$

Kernel-independent acceleration via kernel interpolation

In many cases:

- Fundamental solution available (not necessary ion closed form);
  Availability of high-order derivatives problematic at best
  $\longrightarrow$Taylor-based expansion impractical
- Analytic expansion (e.g. multipole, exponential) not available
  $\longrightarrow$FMM treatment impossible

Idea: **polynomial interpolation** of $G(\mathbf{x},\xi)$ in product of two non-adjacent cells ($\mathbf{x}\in\mathcal{C}_x$, $\boldsymbol{\xi}\in\mathcal{C}_\xi$)

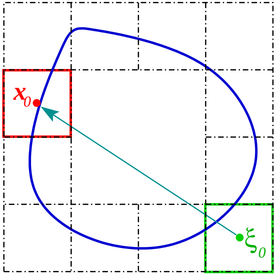

Kernel-independent acceleration via kernel interpolation

$$G(\mathbf{x},\boldsymbol{\xi}) \approx \sum_{p=1}^{P}\sum_{q=1}^{Q} P_p(\mathbf{x})G(\mathbf{x}_p,\boldsymbol{\xi}_q)Q_q(\boldsymbol{\xi})$$

$\mathbf{x}_p$: interpolation nodes in $\mathcal{C}_x$ (Cartesian product of 1-D set of nodes);
$P_p(\mathbf{x})$: interpolation polynomials (e.g. Cartesian product of 1-D Lagrange polyn.);

$\boldsymbol{\xi}_q$: interpolation nodes in $\mathcal{C}_\xi$ (Cartesian product of 1-D set of nodes);
$Q_q(\mathbf{x})$: interpolation polynomials (e.g. Cartesian product of 1-D Lagrange polyn.);

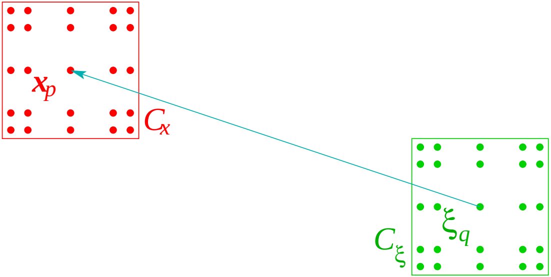

Kernel-independent acceleration via kernel interpolation

Evaluation of

$$\mathcal{S}[\varphi,\partial\Omega]^{\text{far}}(\mathbf{x}) = \sum_{\mathcal{C}_\xi\in\mathcal{A}(\mathcal{C}_x)} \int_{\partial\Omega\cap\mathcal{C}_\xi} G(\mathbf{x},\boldsymbol{\xi})\varphi(\boldsymbol{\xi})\,\mathrm{d}S_\xi$$

- Multipole moments:

$$M_q(\boldsymbol{\xi}_0) = \int_{\partial\Omega\cap\mathcal{C}_\xi} Q_q(\boldsymbol{\xi})\phi(\boldsymbol{\xi})\,\mathrm{d}S_\xi$$

- M2L translation:

$$L_p(\mathbf{x}_0) = \sum_{q=1}^{Q} G(\mathbf{x}_p,\boldsymbol{\xi}_q)M_q(\boldsymbol{\xi}_0)$$

- M2M (upward) translations by expressing the $Q_q^{(\ell-1)}(\boldsymbol{\xi};\boldsymbol{\xi}_0^{(\ell-1)})$ in terms of the $Q_{q'}^{(\ell)}(\boldsymbol{\xi};\boldsymbol{\xi}_0^{(\ell)})$ (e.g. Taylor expansion for polynomials)
- L2L (downward) translations similarly

Adaptive cross approximation

Aim: find recursively a low-rank approximation of a $m \times n$ block $\mathbf{A}$ of the form:

$$\mathbf{A} = \mathbf{R} + \mathbf{S}, \qquad \mathbf{S} = \sum_{k=1}^{r} \mathbf{u}_k \mathbf{v}_k^{\mathsf{T}}, \ \ \|\mathbf{R}\|_{\mathsf{F}} \leq \epsilon$$

To be used in conjunction with a $\mathcal{H}$-matrix block clustering.

- Bebendorf, M., Rjasanov, S.. Adaptive low-rank approximation of collocation matrices. *Computing*, **70**:1–24 (2003).

Adaptive cross approximation: partially-pivoted ACA

1. Initialization: $\mathbf{S} = \mathbf{0}$, $\mathcal{K} = \emptyset$, $r = 0$
2. Recursion:
   (a) $k = \text{Min}\{j, j \notin \mathcal{K}\}$, $\mathcal{K} = \mathcal{K} \cup \{k\}$; **STOP** if $|\mathcal{K}| = n$,
   (b) Row generation: $\mathbf{a} = \mathbf{A}_{k\bullet}$,
   (c) Row of residual, pivot column: $\mathbf{R}_{k\bullet} = \mathbf{a} - \sum_{i=1}^{r} \mathbf{v}_i (\mathbf{u}_i)_k$, $\ell = \text{Argmax}|R_{k\ell}|$,
   (d) Test: if $\text{Max}|R_{k\ell}| = 0$, go to 2(a),
   (e) Column generation: $\mathbf{a} = \mathbf{A}_{\bullet\ell}$,
   (f) Column of residual, pivot row: $\mathbf{R}_{\bullet\ell} = \mathbf{a} - \sum_{i=1}^{r} \mathbf{u}_i (\mathbf{v}_i)_\ell$, $k = \text{Argmax}|R_{k\ell}|$,
   (g) New vectors: $\mathbf{u}_{m+1} = (R_{k\ell})^{-1} \mathbf{R}_{\bullet\ell}$, $\mathbf{v}_{m+1} = \mathbf{R}_{k\bullet}$,
   (h) Stopping criterion: $\|\mathbf{u}_{r+1}\|_{\text{F}} \|\mathbf{v}_{r+1}\|_{\text{F}} \leq \epsilon \|\mathbf{S}\|_{\text{F}}$,
   (i) New approximation of block: $\mathbf{S} = \mathbf{S} + \mathbf{u}_{r+1} \mathbf{v}_{r+1}^{\text{T}}$,
   (j) Recursion: $r = r + 1$, go to 2(b)

- Algorithm requires $O(r^2(m+n))$ operations,
- Complete ACA requires $O(N^{1+\delta} \epsilon^{-\delta})$ operations for any $\delta > 0$ if kernel asymptotically smooth

[Kurz, Rain, Rjasanov, 2006]

Example: crack propagation analysis

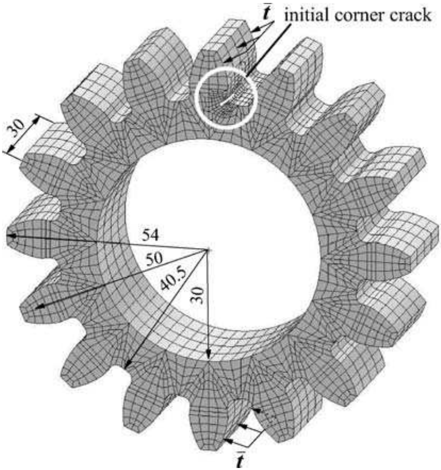

- $N \approx 45000$,
- CPU $\approx$ 4500s
- RAM$=$ 1.5GB

- Kolk, K., Weber, W., Kuhn, G. Investigation of 3D crack propagation problems via fast BEM formulations. *Comp. Mech.*, **37**:32–40 (2005).

- → Diagonal preconditioneur $M_{ij} = A_{ij}\delta_{ij}$;
- → Sparse matrix of near contributions in FMM;
- → Incomplete LU factorization of $\mathbf{A}$;
- → Sparse approximate inverses;
- → Multigrid approaches;
- → Fast BEM solution method (e.g. FMM, ACA) with **low** truncation;
- → Preconditioners exploiting specific features of the problems, e.g. single-inclusion case for many-inclusion problems.

Sparse approximate inverse (SPAI)

- Definition:

$$[A^\sharp] = \arg\min_{[E]} \| \, [I] - [E][A] \, \|_F^2 \qquad [E] \in \mathbb{R}^{N\times N} \text{ sparse}$$

where $[A^\sharp]$ has a **sparsity pattern** (either predefined or found iteratively).

- Hence each column of $[A^\sharp]$ solves an uncoupled, small minimization problem:

$$\{A_k^\sharp\} = \arg\min_{\{E\}} \| \, \{e_k\} - \{E\}[A] \, \| \qquad \{E\} \in \mathbb{R}^{1\times N} \text{ sparse}$$

- **Simplification:** choose number m of nonzero entries in each row of $[A^\sharp]$ and find SPAI of $[\tilde{A}]$:

$$\{\hat{A}_i^\sharp\} = \arg\min_{\{\hat{E}\}\in\mathbb{R}^{1,m}} \Big\{ \| \, \{E\}[\tilde{A}_i] \, \|^2 - 2\,\text{trace}(\{E\}[\tilde{A}_i]) + 1 \Big\} \qquad (1 \leq i \leq N)$$

where $[\tilde{A}]$ is the sparse matrix made of the m largest entries of $[A]$.

Further reading

- BENZI, M.
  Preconditioning techniques for large linear systems: a survey.
  J. Comp. Phys., **182**:418–477 (2002).
- BIROS, G., YING, L., ZORIN, D.
  A fast solver for the Stokes equations with distribuuted forces in complex geometries.
  J. Comp. Phys., **193**:317–348 (2003).
- BONNET, M.
  Boundary Integral Equation Method for Solids and Fluids.
  Wiley (1999).
- BÖRM, S., GRASEDYCK, L., HACKBUSCH, W.
  Introduction to hierarchical matrices with applications.
  Engng. Anal. with Bound. Elem., **27**:405–422 (2003).
- CARPENTIERI, B., DUFF, I. S., GIRAUD, L., SYLVAND, G.
  Combining fast mulrtipole techniques and an approximate inverse precondfitioner for large electromagnetism calculations.
  SIAM J. Sci. Comput., **27**:774–7923 (2005).

- CHAILLAT, S., BONNET, M., SEMBLAT, J. F.
  A multi-level fast multipole BEM for 3-D elastodynamics in the frequency domain.
  Comp. Meth. Appl. Mech. Engng. (2008, in press).
- CHENG, H., CRUTCHFIELD, W. Y., GIMBUTAS, Z., GREENGARD, L. F., ETHRIDGE, J. F., HUANG, J., ROKHLIN, V., YARVIN, N.
  A wideband fast multipole method for the Helmholtz equation in three dimensions.
  J. Comp. Phys., **216**:300–325 (2006).
- CHEW, W. C. ET AL.
  Fast integral equation solvers in computational electromagnetics of complex structures.
  Engng. Anal. with Bound. Elem., **27**:803–823 (2003).
- COIFMAN, R., ROKHLIN, V., WANDZURA, S.
  The Fast Multipole Method for the Wave Equation : A Pedestrian Prescription.
  IEEE Antennas and Propagation Magazine, **35**:7–12 (1993).

- Colton, D., Kress, R.
  Integral Equation Method in Scattering Theory.
  John Wiley and sons (1983).

- Darve, E.
  The fast multipole method: I. Error analysis and asymptotic complexity.
  SIAM J. Numer. Anal., **38**:98–128 (2000).

- Darve, E.
  The fast multipole method: numerical implementation.
  J. Comp. Phys., **160**:195–240 (2000).

- Darve, E., Havé, P.
  Efficient fast multipole method for low-frequency scattering.
  J. Comp. Phys., **197**:341–363 (2004).

- Dominguez, J.
  Boundary elements in dynamics.
  Comp. Mech. Publ., Southampton (1993).

- Epton, M.A., Dembart, B.
  Multipole translation theory for the three-dimensional Laplace and Helmholtz equations.
  SIAM J. Sci. Comp., **16**:865–897 (1995).
- Ergin, A. A., Shanker, B., Michielssen, E.
  Fast evaluation of three-dimensional transient wave fields using diagonal translation operators.
  J. Comp. Phys., **146**:157–180 (1998).
- Fischer, M., Gaul, L.
  Application of the fast multipole bem for structural-acoustic simulations.
  Journal of Computational Acoustics, **13**:87–98 (2005).
- Fochesato, C., Dias, F.
  A fast method for nonlinear three-dimensional free-surface waves.
  Proc. Roy. Soc. A, **462**:2715–2735 (2006).
- Frayssé, V., Giraud, L., Gratton, S., Langou, J.
  A Set of GMRES Routines for Real and Complex Arithmetics on High Performance Computers.
  Tech. rep., CERFACS (2003).

- Fu, Y., Klimkowski, K. J., Rodin, G. J., Berger, E., Browne, J. C., Singer, J. R., van der Greijn, R. A., Vemaganti, K. S.
  A fast solution method for the three-dimensional many-particle problems of linear elasticity.
  Int. J. Num. Meth. in Eng., **42**:1215–1229 (1998).
- Fujiwara, H.
  The fast multipole method for the integral equations of seismic scattering problems.
  Geophys. J. Int., **133**:773–782 (1998).
- Fujiwara, H.
  The fast multipole method for solving integral equations of three-dimensional topography and basin problems.
  Geophys. J. Int., **140**:198–210 (2000).
- Greenbaum, A.
  Iterative methods for solving linear systems.
  SIAM, Philadelphia, USA (1997).

- Greengard, L., Huang, J., Rokhlin, V., Wandzura, S.
  Accelerating fast multipole methods for the Helmholtz equation at low frequencies.
  IEEE Comp. Sci. Eng., **5**:32–38 (1998).
- Greengard, L., Rokhlin, V.
  A fast algorithm for particle simulations.
  J. Comp. Phys., **73**:325–348 (1987).
- Greengard, L., Rokhlin, V.
  A new version of the fast multipole method for the Laplace equation in three dimensions.
  Acta Numerica, **6**:229–270 (1997).
- Gumerov, N. A., Duraiswami, R.
  Fast multipole methods for the Helmholtz equation in three dimensions.
  Elsevier (2005).
- Hackbusch, W., Nowak, Z. P.
  On the fast matrix multiplication in the boundary element method by panel clustering.
  Numerische Mathematik, **54**:463–491 (1989).

- HACKBUSCH, W., WITTUM, G. (eds.).
  Boundary elements: implementation and analysis of advanced algorithms.
  Wieweg, Braunschweig (1996).

- JIANG, L. J., CHEW, W. C.
  A mixed-form fast multipole algorithm.
  IEEE Trans. Antennas Propagat., **53**:4145–4156 (2005).

- KELLOGG, O.D.
  Fundations of potential theory (1929).

- KOLK, K., WEBER, W., KUHN, G.
  Investigation of 3D crack propagation problems via fast BEM formulations.
  Comp. Mech., **37**:32–40 (2005).

- KUPRADZE, V.D.
  Dynamical problems in elasticity.
  North-Holland, p. 259 (1963).

- KURZ, S., RAIN, ; O., RJASANOW, S.
  The adaptive cross approximation technique for the 3D boundary element method.
  IEEE Transactions on Magnetics, **38**:421–424 (2002).

- Lage, C., Schwab, C.
  Wavelet Galerkin algorithms for boundary integral equations.
  SIAM J. Sci. Comput., **20**:2195–2222 (1999).
- Liu, Y., Nishimura, N.
  The fast multipole boundary element method for potential problems: a tutorial.
  Engng. Anal. with Bound. Elem., **30**:371–381 (2006).
- Liu, Y., Nishimura, N., Otani, Y., Takahashi, T., Chen, X. L., Munakata, H.
  A fast boundary element method for the analysis of fiber-reinforced composites based on a rigid-inclusion model.
  ASME J. Appl. Mech., **72**:115–128 (2005).
- Margonari, M., Bonnet, M.
  Fast multipole method applied to the coupling of elastostatic BEM with FEM.
  Computers and Structures, **83**:700–717 (2005).
- Martinsson, P. G., Rokhlin, V.
  A fast direct solver for boundarry integral equations in two dimensions.
  J. Comp. Phys., **205**:1–23 (2005).

- NÉDÉLEC, J. C.
  Acoustic and electromagnetic equations.
  Applied mathematical sciences (vol. 144). Springer Verlag (2001).
- NEMITZ, N., BONNET, M.
  Topological sensitivity and FMM-accelerated BEM applied to 3D acoustic inverse scattering.
  Engng. Anal. with Bound. Elem. (2008).
- NISHIMURA, N.
  Fast multipole accelerated boundary integral equation methods.
  Appl. Mech. Rev., **55**:299–324 (2002).
- ROKHLIN, V.
  Rapid solution of integral equations of classical potential theory.
  J. Comp. Phys., **60**:187–207 (1985).
- ROKHLIN, V.
  Rapid solution of integral equations of scattering theory.
  J. Comp. Phys., **86**:414–439 (1990).

- ROKHLIN, V.
  Diagonal forms of translation operators for the Helmholtz equation in three dimensions.
  Appl. Comp. Harmonic Anal., **1**:82–93 (1993).
- ROKHLIN, V.
  Sparse diagonal forms for translation operators for the Helmholtz equation in two dimensions.
  Appl. Comp. Harmonic Anal., **5**:36–67 (1998).
- SAAD, Y.
  Iterative methods for sparse linear systems.
  SIAM (2003).
- SAAD, Y., SCHULTZ, M.H.
  GMRES: a generalized minimal residual algorithm for solving nonsymmetric linear systems.
  SIAM J. Sci. Stat. Comput., **7**:856–869 (1986).

- Sakuma, T., Yasuda, Y..
  Fast multipole boundary element method for large-scale steady-state sound field analysis. Part I: setup and validation.
  Acta Acustica united with Acustica, **88**:513–525 (2002).
- Schmindlin, G., Lage, C., Schwab, C.
  Rapid solution of first kind boundary integral equations in $\mathbb{R}^3$.
  Engng. Anal. with Bound. Elem., **27**:469–490 (2003).
- Song, J., Lu, C.C., Chew, W.C.
  Multilevel fast multipole algorithm for electromagnetic scattering by large complex objects.
  IEEE Trans. Antennas Propag., **42**:1488–1493 (1997).
- Sylvand, G.
  La méthode multipôle rapide en éléctromagnétisme : performances, parallélisation, applications.
  Ph.D. thesis, ENPC (2002).

- TAKAHASHI, T., KAWAI, A., EBISUZAKI, T.
  Accelerating boundary-integral equation method using a special-purpose computer.
  Int. J. Num. Meth. in Eng., **66**:529–548 (2006).
- TAKAHASHI, T., NISHIMURA, N., KOBAYASHI, S.
  A fast BIEM for three-dimensional elastodynamics in time domain.
  Engng. Anal. with Bound. Elem., **28**:165–180 (2004).
- TAUSCH, J.
  Sparse BEM for potential theory and Stokes flow using variable order wavelets.
  Comp. Mech., **32**:312–3185 (2003).
- WANG, P. B., YAO, Z. H..
  Fast multipole DBEM analysis of fatigue crack growth.
  Comp. Mech., **38**:223–233 (2006).
- YARVIN, N., ROKHLIN, V.
  Generalized Gaussian quadratures and singular value decompositions of integral operators.
  SIAM J. Sci. Comput., **20**:699–718 (1997).

- YING, L., BIROS, G., ZORIN, D.
  A kernel-independent adaptive fast multipole in two and three dimensions.
  J. Comp. Phys., **196**:591–626 (2004).
- YOSHIDA, K.I.
  Applications of fast multipole method to boundary integral equation method.
  Ph.D. thesis, University of Kyoto (2001).
- YOSHIDA, S., NISHIMURA, N., KOBAYASHI, S.
  Application of fast multipole Galerkin boundary integral equation method to elastostatic crack problems in 3D.
  Int. J. Num. Meth. in Eng., **50**:525–547 (2001).